NTNU – Trondheim
Norwegian University of
Science and Technology

The B7-H3 Protein and its role in Breast Cancer Treatment Response

Cathrine Pedersen

Biotechnology (5 year)

Supervisor: Svein Valla, IBT
Co-supervisor: Kristine Kleivi, Radiumhospitalet

Norwegian University of Science and Technology
Department of Biotechnology

Acknowledgments

The work presented in this thesis has been carried out at the Department of Genetics and at the Department of Tumor Biology, Institute for Cancer Research at The Norwegian Radium Hospital in Oslo from 2011 to 2012.

I would like to express my gratitude to Professor Anne-Lise Børresen-Dale, head of the Department of Genetics, for providing the research facilities and opening doors to Master students. Also, I would like to express my sincere gratitude to my supervisor, Dr Kristine Kleivi, for good scientific guidance, follow up and support, and for providing such an exciting thesis. A special thanks to my co-supervisor Dr Christina Tekle for guidance both in the laboratory and with scientific questions. I have enjoyed working with you, and you have always been encouraging and enthusiastic. I am also grateful to Professor Svein Valla at NTNU for taking care of all the formalities during this thesis.

Furthermore, I would like to thank Sandra Nyberg and Dagim S. Tadele for teaching me and helping me in the laboratory, and Hege Edvardsen for encouraging inputs. I wish to express gratitude to all colleagues and friends in the Department of Genetics for help and support. You have made me feel very welcome here, and you create a positive and enjoyable working environment.

Last, but not the least, I would like to share my deepest gratitude to all my fellow students at NTNU for making the past five years such an important part of my life. Especially Tone, I am so lucky to have you to share my joys, frustrations and journey here in Oslo with. Also, I must give a special thanks to my mom and dad who has always supported me, and my sister, brother, grandfather and friends back in Tromsø, who gives me so much in life.

Oslo, Mai 2012

Cathrine Pedersen

Table of Contents

Acknowledgments 1
Abstract 4
Sammendrag 5
Aim of study 6
1.Introduction 7
1.1 Cancer 7
1.2 Breast cancer 9
1.2.1 Breast cancer incidence and risk factors 9
1.2.2 The human breast anatomy and breast cancer development 11
1.3 Diagnosis, classification and treatment of invasive breast cancer 12
1.3.1 Tumors staging according to the TNM classification 13
1.3.2 Histological grade 14
1.3.3 Receptor status 14
1.3.4 Treatment 15
1.4 The metastatic process 16
1.5 Signal transduction in breast cancer 20
1.6 Resistance to anti-cancer drugs 22
1.7 The B7-H3 protein, a member of the B7/CD28 family of co-stimulatory proteins 23
2. Material and methods 26
2.1 Breast cancer cell lines 26
2.2 Cell culturing 26
2.3 Cell counting using hemocytometer 28
2.4 The Cell titer glo® (CTG) Luminescent cell viability assay 28
2.5 Optimizing of cell lines for growth in 384 well plates 29
2.6 Drug screening of B7-H3 expressing and B7-H3 silenced breast cancer cell lines 30
2.6.1 Description of the drugs screened and plate annotation. 30
2.6.2 The drug screening procedure in 384 well plates 32
2.7 Statistical analyses and growth inhibition curves 33
2.8 Treatment of MDA-MB-231 and MDA-MB-435 cell variants with API-2 and Everolimus 34
2.9 Harvesting of cells 34
2.10 Cell lysis 35
2.11 Measuring protein concentrations by the BCA assay 36
2.12 Western blot 37

3. Results 43
3.1 Optimization of cell lines 43
3.2 Drug screening of breast cancer cells 44
3.2.1 Drug response in MDA-MB-435 cell variants 46
3.2.2 Drug response in MDA-MB-231 cell variants 47
3.2.3 The half maximal effective concentration (EC_{50}) 49
3.3 Confirmation of B7-H3 silencing in MDA-MB-435 and MDA-MB-231 cell variants 49
3.4 Western blot analysis of target proteins in the PI3K/AKT pathway 50
3.4.1 MDA-MB-435 cells treated with API-2 (20 µM) 51
3.4.2 MDA-MB-231 cells treated with API-2 (2µM) 51
3.4.3 MDA-MB-231 cells treated with Everolimus (200 nM) 52
4. Discussion 54
4.1 Methodological considerations 54
4.1.1 *In Vitro* cell cultures 54
4.1.2 The origin of cell line MDA-MB-435 55
4.1.3 Drug screening of breast cancer cell lines 56
4.1.4 Western blot analysis of proteins 58
4.2 Biological considerations 60
5. Conclusion 70
6. Future perspectives 71
APPENDIX A: Reagents and equipment 82
APPENDIX B: Preparation of Lysis Buffer (LB) and Bovine Serum Albumin (BSA) Standard 84

Abstract

Breast cancer is the most common cancer type amongst women, and closer to 3000 women in Norway will be diagnosed with this disease in 2012. Although major improvements have been achieved in the treatment, and thus the outcome, of breast cancer patients in the past years, little has been accomplished for those with an advanced disease.

B7-H3 is an immunoregulatory protein, and its overexpression has been associated with advanced disease and poor prognosis in breast cancer. A previous study has shown that B7-H3 silencing increased Paclitaxel sensitivity in B7-H3 expressing breast cancer cell lines. Resistance to treatment is a general challenge in systemic management of advanced breast cancer, and increased knowledge about the molecules and pathways involved in this process is important in order to improve the outcome for these patients.

To further study the function of B7-H3 and its putative involvement in lack of treatment response in breast cancer, we compared the efficacy of 22 different anti-cancer drugs in two B7-H3 expressing triple negative metastatic breast cancer cell lines, MDA-MB-435 and MDA-MB-231, and their B7-H3 silenced counterparts. In particular two drugs targeting the PI3K/Akt pathway, API-2 and Everolimus, showed a significantly better efficacy in the B7-H3 silenced cells.

To elucidate the cellular mechanisms involved in the observed sensitization in the B7-H3 knockdown cells, we performed Western blot analysis on several proteins in the PI3K/Akt/mTOR pathway. The cells that did not express B7-H3 had lower levels of both phospho-Akt and the downstream signaling molecule phospho-p70S6K following drug exposure, indicating B7-H3 associated the regulation of proteins in this pathway. This, together with the previously observed relationships between B7-H3 expression in metastasis and chemoresistance, suggest that this protein might be a therapeutic marker to increase the effect of current anti-cancer treatment, although the specific roles of B7-H3 in this context need to be investigated further.

Sammendrag

Brystkreft er den vanligste krefttypen blant kvinner i Norge. Selv om store fremskritt har blitt gjort i behandlingen de seneste årene, er prognosen fortsatt dårlig for de pasientene der sykdommen har spredd seg. B7-H3 er et immunoregulatorisk protein, og høyt uttrykk er forbundet med spredning og dårlig prognose i flere krefttyper, deriblant i brystkreft. Oppregulert B7-H3 har også blitt forbundet med resistens mot kjemoterapi i brystkreft cellelinjer. Resistens mot behandling er en stor utfordring innen kreftbehandling, og da særlig hos pasienter hvor sykdommen har spredd seg. Økt kunnskap om molekyler og underliggende mekanismer for resistens er derfor viktig for å kunne bedre behandlingen og overlevelsen av brystkreft pasienter.

Vi ønsket å ytterligere undersøke den observerte sammenhengen mellom et høyt uttrykk av B7-H3 og mangelen på behandlingsrespons i brystkreft. Dette ble gjort ved å sammenligne effekten av 22 forskjellige anti-cancer medikamenter i to trippel negative metastatiske brystkreftcellelinjer MDA-MB-435 og MDA-MB-231 som uttrykte B7-H3 og som ikke uttrykte dette proteinet. Vi identifiserte to små molekyl-hemmere, API-2 og Everolimus, som hadde bedre effekt i kreft cellene som hadde lavt B7-H3 uttrykk.

Western blot analyser ble utført for å finne ut mer om de molekylære mekanismene bak den observerte B7-H3 medierte sensitivering. Ved å undersøke aktivitetsnivået av flere proteiner i PI3K/Akt signalveien, som spesifikt blir inhibert av disse hemmerene, så vi at celler som ikke uttrykte B7-H3 hadde lavere nivåer av både fosforylert Akt (aktiv form) og et molekyl nedstrøms for Akt, fosforylert p70S6K. Nedsatt aktivitet av denne signalveien fører til redusert cellevekst, og våre resultater indikerer at B7-H3 medierer, indirekte eller direkte, regulering av proteiner i denne signalveien. Dette, tatt i betraktning med den tidligere observerte sammenhengen mellom høyt B7-H3 uttrykk og metastase og kjemoresistens tyder på at proteinet kan være et mulig terapeutisk mål som kan øke sensitiviteten til dagens kreftmedikamenter, men den spesifikke rollen til B7-H3 i denne sammenhengen må imidlertid undersøkes nærmere.

Aim of study

Resistance to treatment is a general challenge in breast cancer therapy, and increased knowledge about the underlying mechanisms and the identification of new therapeutic markers are important in order to improve patient outcome.

B7-H3 is an immunoregulatory protein, and a high expression of this protein has been associated with advanced disease and poor prognosis in breast cancer, as well as in other types of cancer. The exact physiological role is not known, but a recent study showed that knockdown of B7-H3 increased the sensitivity to Paclitaxel in breast cancer cell lines *in vitro* and *in vivo*. The aim of the present thesis was to further study the role of B7-H3 in treatment response in breast cancer, in particular by;

1. Further investigating the role of B7-H3 in drug resistance by performing a drug screen of B7-H3 knockdown breast cancer cell lines and their B7-H3 expressing counterparts. The drug screen constituted a panel of 22 anti-cancer drugs, both chemotherapeutics and small molecule inhibitors,
2. Elucidating the underlying mechanisms behind any B7-H3 induced difference in drug efficacy obtained from the drug screen by performing Western blot analysis of target proteins.

1. Introduction

1.1 Cancer

Cancer is a broad group of diseases and is characterized by uncontrolled cell growth. The abnormal cells may grow and divide, leading to the formation of a clump of cells, a tumor, that can be benign (not cancer) or malignant (cancer). A malignant tumor can divide and invade the surrounding tissue, and some of the cancer cells may spread through the blood stream or the lymphatic system and form tumors at distant sites of the body, a process called metastasis (1). Benign tumors lack the invasive and metastatic capacity of malignant tumors; however the abnormal growth may damage local tissue. A cancer is named after its tissue of origin, and thus a breast cancer that has spread to in example the lung is called metastatic breast cancer (2). This is because it continues to grow as a breast cancer in the foreign tissue, and this is of importance with respect to treatment selection. In 2008, there was an estimate of 12.7 million new cancer cases around the world, where the most common forms were lung, breast (in women) and colorectal cancer (3;4).

Cancer is a genetic disease where several genetic and epigenetic alterations are required for its development and progression (5;6). Genes encoding tumor suppressor genes, oncogenes and DNA repair genes are frequently mutated, as they are involved in mechanisms that orchestrate normal tissue growth (1). In addition, epigenetic alterations and small micro-RNA (miRNA) changes also contributes to the development of the disease (1;7).

The process of tumorgenesis, the initiation and development of a tumor, is a multistep process where the cell gains genetic alterations followed by natural selection of its progenies with advantageous mutations. This drives the transformation of normal human cells to progressively more malignant progenies (8). Several hypotheses have been suggested regarding tumorgenesis and the origin of tumor heterogeneity (9). *Nowell* proposed that tumor development occurs through the clonal expansion of one malignant cell that, by sequential proliferation, gives rise to a heterogeneous tumor. In this theory, all progenies have the ability to promote sustained proliferative signaling,

and thus are able to propagate the tumor (10). Another hypothesis of tumor initiation and development is the cancer stem cell (CSC) theory (11), where a malignant cell with stem cell-like properties, the capacity of unlimited self-renewal, has a high tumorigenic potential (tumor initiating properties). This cell has the ability to form a heterogeneous tumor mass by asymmetric cell division, where the progenies display non-tumorigenic potential (11). According to this theory, the CSCs thus represent the small bulk of the tumor responsible for its propagation (12;13). In addition, the polyclonal evolution model, the self-seeding model and the mutator phenotype model of tumor progression and heterogeneity add additional layers of complexity to the biology of cancer. Importantly, studies supporting all these models imply that different cancers may evolve by several mechanisms (9).

Although cancer is a heterogeneous and complex disease, there are several central capabilities that most, if not all, cancers acquire. In 2000, Hanahan and Weinberg proposed six alterations in cell physiology essential for malignant growth referred to as the hallmarks of cancer. These acquired capabilities are: 1) sustained proliferative signaling, 2) evasion of growth suppressing signals, 3) resisting cell death, 4) enabling replicative immortality, 5) inducing angiogenesis and 6) activating invasion and metastasis (8). In 2011, the same authors described two additional emerging hallmarks; the ability to reprogram the energy metabolism and the evasion of immune destruction. Moreover, they defined two categories of enabling characteristics which both facilitate the acquisition of core- and emerging hallmarks, as well as serving as a driving force in tumor development: genome instability and mutation and tumor-promoting inflammation. The authors also acknowledge the contribution of the tumor microenvironment in cancer (14). These conceptual hallmarks serve as a framework in cancer biology, and are illustrated in Figure 1.

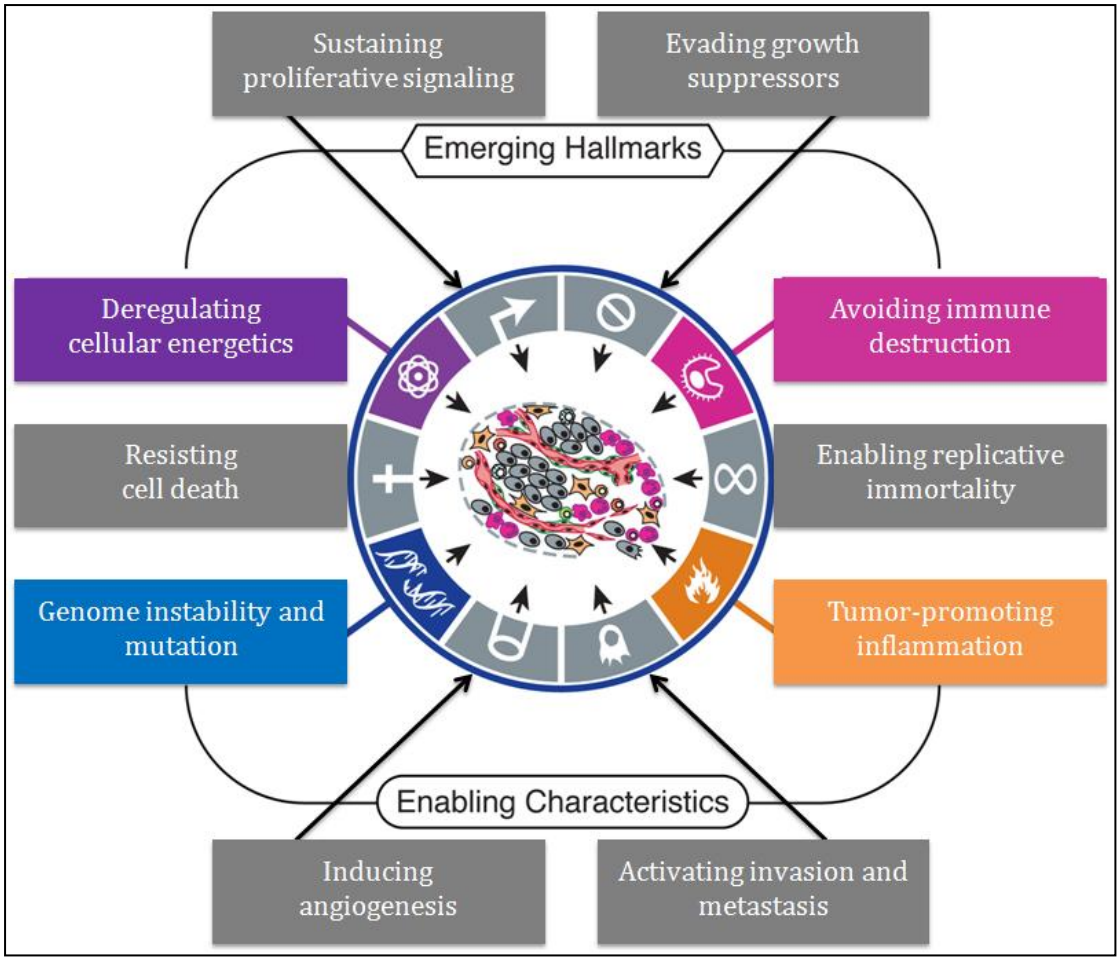

Figure 1. The hallmarks of cancer. The hallmarks of cancer are common traits that cancer cells must acquire to have the biological capacity for malignant growth as proposed by Hanahan and Weinberg. Central to acquiring and facilitating these cancerous properties are the enabling characteristics and the interaction with the microenvironment (modified from (14)).

1.2 Breast cancer

1.2.1 Breast cancer incidence and risk factors

Breast cancer is the most common type of cancer in women worldwide with 1.4 million new cases diagnosed in 2008 (4). In Norway, close to 3000 patients are diagnosed with this disease every year. Major development in cancer treatment and early detection can explain the high relative survival rate of 88 % in breast cancer patients (15). Early detection by mammographic screening might have an impact on the improved prognosis through discovering more breast cancer at a less advanced stage, though its putative impact on survival has not yet been confirmed. The breast cancer tumors are classified into different stages (from I to IV) according to their

aggressiveness. Despite the improvements in cancer care, little has been accomplished for the patients that have metastatic disease at the time of diagnosis (Stage IV), and these patients still have a poor 5-year survival (15) (Figure 2).

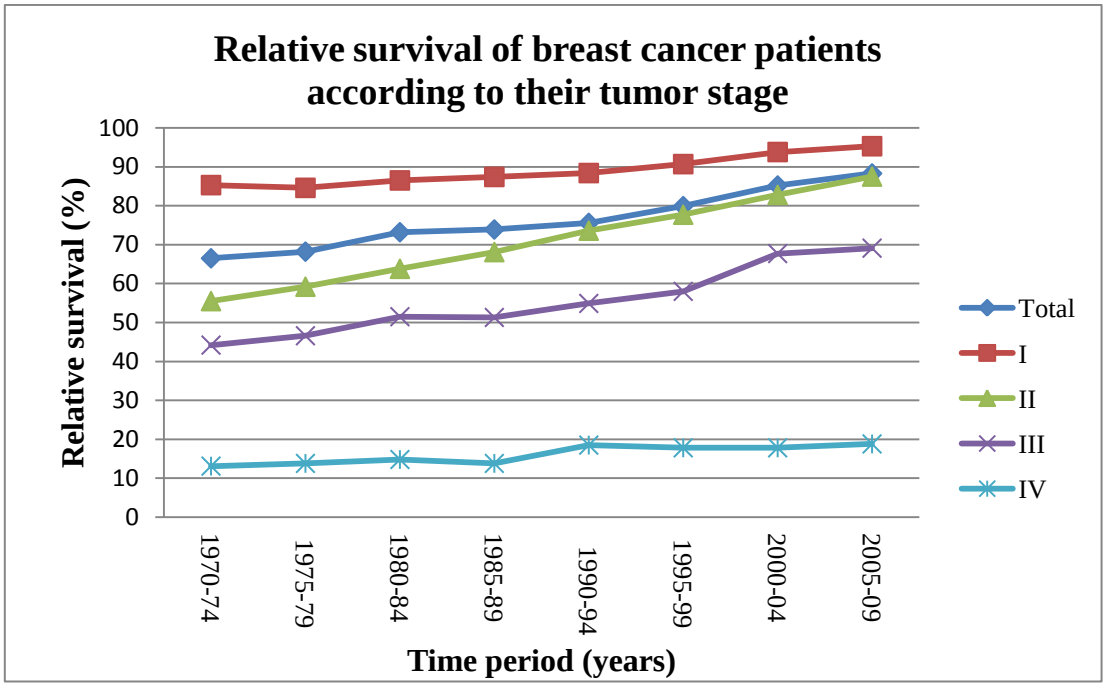

Figure 2. The relative 5-year survival of breast cancer patients in Norway from 1970 to 2009 according to their tumor stage. The stage of the tumor refers to the extent of the disease based on several factors, with a higher tumor stage the more advanced the disease is. Notice that the patients with tumors stage IV (metastatic disease) have little, if any, change in relative survival from 1970 to present day (The Figure is based on data from the Cancer registry of Norway (15)).

The etiology of breast cancer is multifactorial, with multiple genetic, hormonal and environmental factors contributing to the risk of developing the disease. Hereditary breast cancer accounts for approximately 5-10 % of all breast cancer, thus the majority of breast cancer arises somatically (6). The hormonal risk factors are many, including age, early onset of menarche, late menopause and not having breast fed (16;17). All these factors contribute to the risk of breast cancer development due to prolonged exposure to the hormone estrogen (17). In addition environmental factors, such as carcinogens and UV exposure, and life style factors, such as low physical exercise and obesity, all contribute to the risk of developing breast cancer (15;16). In post-menopausal women, estrogen is synthesized by fat cells (adipocytes), and obesity may therefore lead to an elevated estrogen exposure (17).

1.2.2 The human breast anatomy and breast cancer development

The human breast, or mammary gland, is situated on the rib cage above the *Pectoralis major* muscle, and the organ's main function is to produce milk (18;19) (Figure 3). In the mammary gland the major developmental steps occur after birth and are related to puberty and reproduction (19). The mammary epithelial growth and development are regulated through growth hormone (GH), estrogen, progesterone and prolactin (19). The breast has glandular tissue consisting of 15-20 lobes, which are composed of many smaller structures named lobules. The lobules produce milk upon hormonal stimuli which is secreted through the ducts to the nipple (18). The ducts and the lobules have an inner layer of epithelial cells, surrounded by an outer layer of myoepithelial cells that are separated from the stroma by the basement membrane (19). The stroma consists mainly of adipose tissue, but also a variety of other cells and an infiltrating network of lymphatic vessels and nodes, in addition to blood vessels that remove waste and provide nutrition's and oxygen to the tissue (19;20).

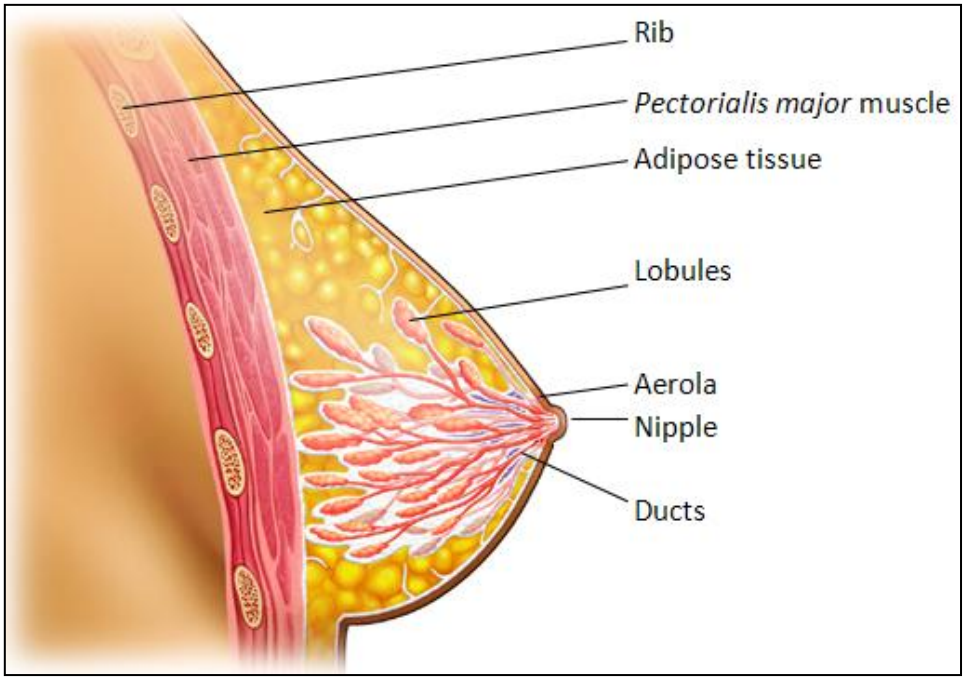

Figure 3. The human breast anatomy. The structure of the female breast is mainly composed of fat, but also glandular tissue (adapted from (21)).

Breast cancer is divided into two main categories: carcinomas in situ (CIS), which are enclosed by the basement membrane, and invasive carcinomas (IC). CIS may eventually develop to IC, and is considered the precursor of invasive cancer (2;22). IC

is generally separated into two main types: invasive ductal carcinoma (IDC) and invasive lobular carcinoma (ILC) which arises in the epithelial cells in the ducts or lobules of the breast, respectively. Several other subtypes exist, however IDC and ILC account for the majority with 70-80 % and 10-20 % of all invasive carcinomas, respectively (23). The progression of breast cancer will here be exemplified by the development of IDC, as this is the most common malignancy (Figure 4). DC develops through sequential steps from atypical hyperplasia, a premalignant lesion of abnormal cells within the ducts, to ductal carcinoma in situ (DCIS), a non-invasive lesion of cancer cells. At this point the tumor is still encapsulated by the basement membrane (24). The next step is characterized by the degradation of the basement membrane and invasion to the surrounding tissue, and some tumor cells may eventually progress to become metastatic (5).

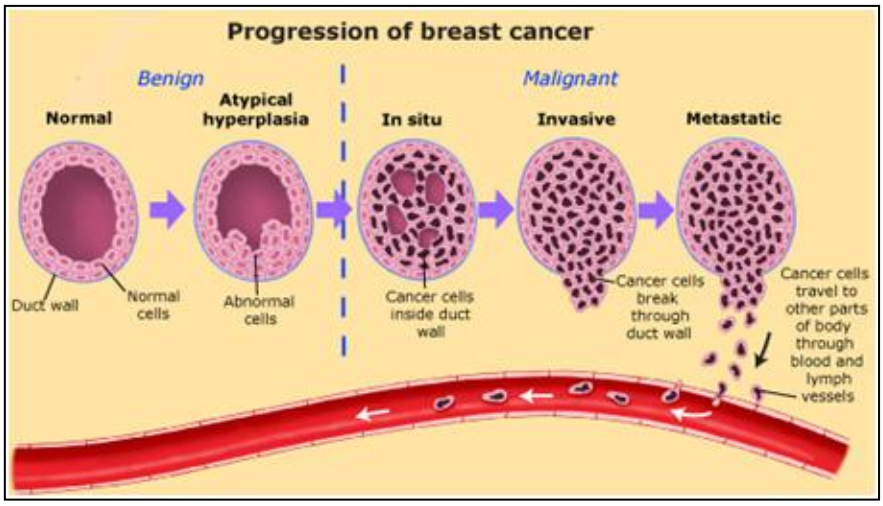

Figure 4. The multistep development of cancers in the ducts of the breast. The normal breast has ducts composed of an organized lining of epithelial cells that are surrounded by a basement membrane. Breast cancer is thought to progressively develop through *in situ* and invasive to metastatic cancer (available from (25)).

1.3 Diagnosis, classification and treatment of invasive breast cancer

Breast cancer is a broad group of diseases, as confirmed by molecular profiling studies which classified breast cancer into five distinct subgroups based on their genetic composition: Luminal A (ER+), Luminal B (ER+), *ERBB2*-enriched (HER2+), Basal-like and Normal-like tumors (26;27). Importantly, each subclass

showed different clinical outcomes (27). Current treatment of breast cancer appreciates the diversity of the disease, and patients are evaluated with regard to age and tumor characteristics to help guide the treatment. Still, the identification of new therapeutic and prognostic markers is important in order to identify the patients who will benefit from treatment, and to improve the outcome for patients with aggressive disease.

In Norway, the diagnosis of breast cancer is based on the "triple test". This test consists of a clinical examination, radiographic imaging (by mammography, ultrasound or MR), and a pathology test (either by fine needle aspiration or core needle biopsy). Tumors are pathologically evaluated and classified according to three distinct categories: tumor stage (by the TNM standard), histological grade and receptor status (the presence of the estrogen receptor, the progesterone receptor or the HER2 receptor), in addition to the expression of the proliferation marker Ki67 (23). Together, the information of these parameters has prognostic and predictive value, and is used to stratify individual patients for appropriate treatment according to guidelines provided by the Norwegian Breast Cancer Group (NBCG) (23).

1.3.1 Tumors staging according to the TNM classification

The staging of a breast tumor is performed on the basis of the TNM (Tumor, Node and Metastasis) classification system provided by the American Joint Committee on Cancer (AJCC) (28). The TNM staging combines information based on three characteristic features of malignant tumors: the primary tumor size (T), the regional lymph node status (N), and whether the tumor has spread to a distant organ (M). The T category is given a number from 1 to 3 with increasing tumor size. The N (the regional lymph node status) category is assigned a value from 1 to 3 increasing with the number of positive regional lymph nodes, and the M (metastasis) value describes whether the tumor has spread to other parts of the body (M1) or not (M0). These three parameters of the TNM system are combined to a tumor stage that ranges from 0 to IV (metastatic disease) (28). The different stages are important prognostic factors with lower tumor grade indicating a better survival (29).

1.3.2 Histological grade

The histological grade, or tumor grade, is a measure of the tumor cells' proliferation and differentiation and is based on three morphological features. These are the percentage of tubule formation, the degree of nuclear pleomorphism and an accurate mitotic count (30;31). Each feature is given a value which is summed in the total score ranging from 1-3. The different grades indicate how differentiated the tumor cells are: grade 1 which are highly differentiated tumor cells (good prognosis) to grade 3 which are poorly differentiated tumor cells (poor prognosis) (31). The tumor grade is, together with tumor size and lymph node metastasis status, the most important prognostic indicator for predicting the risk of distant metastasis, and thus when considering systemic adjuvant treatment (treatment in addition to and after surgery) (23).

1.3.3 Receptor status

Breast cancer tumors are classified according to their expression of the two hormonal receptors, the Estrogen (ER) and the Progesterone receptors (PR), in addition to the growth factor receptor HER2. The evaluation of these receptors are of clinical importance for treatment decision as substances targeting specific receptors have been developed (23). Tumors with a high expression of these receptors are called ER positive (ER+), PR positive (PR+) or HER2 positive (HER2+), respectively. Patients with ER+/PR+ tumors have the lowest risk of mortality compared to ER-/PR- tumors (32), and hormonal receptor status is therefore a positive prognostic marker. About 20 % of breast cancer patients overexpress the HER2 receptor. Their clinical course is generally aggressive, and the expression of this protein is thus a marker of poor prognosis (33). However, the development of treatment targeting this receptor has improved the prognosis of this patient group (34). In addition, Ki-67 is used as a prognostic marker to evaluate the proliferative activity of breast cancer. This protein marker is present in all proliferative cells, and a high expression is associated with a higher risk of relapse and worse survival in breast cancer patients (35).

1.3.4 Treatment

Treatment of breast cancer patients in Norway is administered according to the guidelines established by the NBCG, and is based on the patient's age, genetic predisposition and the tumor classifications described above. The standard treatment of breast cancer include surgery, radiation therapy, chemotherapy, hormone therapy and HER2 targeted treatment (23). In general, combinations of these therapies are administered.

The primary treatment of breast cancer is usually surgery, however, this is limited by both the location and size of the tumor. A main challenge in cancer treatment is the relapse of the primary tumor or the occurrence of distant metastasis after surgery. The tumor classification described above is an important tool to identify these patients, and to decide adjuvant treatment.

Both radiation therapy and chemotherapy can be used neo-adjuvant (before surgery) to shrink the tumor to an operable size, adjuvant to kill any residual cancer cells after surgery or as palliative treatment (23). Radiation therapy uses a high energy beam directed to the area where the cancer cells may reside after surgery. This beam induces damage to the DNA of cancerous cells as well as normal cells, and is thus not selective. However, cancer cells are rapidly dividing, less differentiated and often have a reduced/defect DNA-repair system. Hence, they are more affected by the damage induced by radiation compared to normal cells, and this therapy has been shown to reduce the risk of recurrence and increase overall survival in breast cancer patients (36;37).

Chemotherapy inhibits replication, cell division or DNA repair, thus attacking key features of the rapidly dividing cancer cells (38). However, the treatment is systemic, and therefore normal cells that are rapidly dividing are also affected. This gives rise to the adverse side effects of chemotherapy such as hair loss, fatigue, nausea and decreased production of blood cells. Women with positive receptor status are treated with targeted therapy, such as the anti-estrogen Tamoxifen or aromatase inhibitors for ER+ breast cancer patients, and the monoclonal antibody Trastuzumab for HER2 positive breast cancer patients (23). Importantly, these therapies are directed towards

specific features of the cancer cell, minimizing the adverse side effects of conventional therapies. However, approximately 12-17 % of all breast tumors do not express the ER, PR or HER2 receptors, and are called triple negative (39). Hormonal treatment and HER2 targeted treatment is not an option for these patients, and the management is limited to conventional therapy (39). There is a high rate of local and systemic relapse associated with the patients with triple negative breast cancer (23;40;41), and this group is characterized by adverse prognosis and an aggressive clinical course (39;41;42), emphasizing the importance of identifying new therapeutic markers that could improve their clinical outcome.

1.4 The metastatic process

Metastasis, the dissemination of cells from the primary tumor and establishment of growth at a secondary, distant site, accounts for 90 % of all cancer related deaths (43;44). While a non-invasive primary tumor can be surgically resected, metastatic disease is almost impossible to eradicate by surgery or local irradiation also frequently develops resistance to the therapy given (1).

Several alterations in the cancer cells' physiology, as well as a dynamic interaction with the microenvironment, is required in the process of metastasis (14)**.** The metastatic cascade of solid tumors is describes as a series of sequential, interlinked and stochastic steps (45), as illustrated in Figure 5. These include the loss of adhesion molecules and degradation of the basement membrane, following infiltration of the extracellular matrix. Next, the cancer cell must enter the blood and/or lymphatic system (intravasate) where it must both survive mechanical stress and evade destruction by the immune system. Subsequently, the cell must be able to arrest in the circulation at a distant organ and exit from the vasculature into the tissue (extravasate). To colonize, the cancer cell must adapt to the tissue, establish growth and induce angiogenesis (44;46). Importantly, in order for a metastasis to occur, all the above mentioned steps in the cascade need to be fulfilled, making metastasis a highly inefficient process. A minority of the cells that disseminate from the primary tumor will successfully establish growth at a secondary site (47).

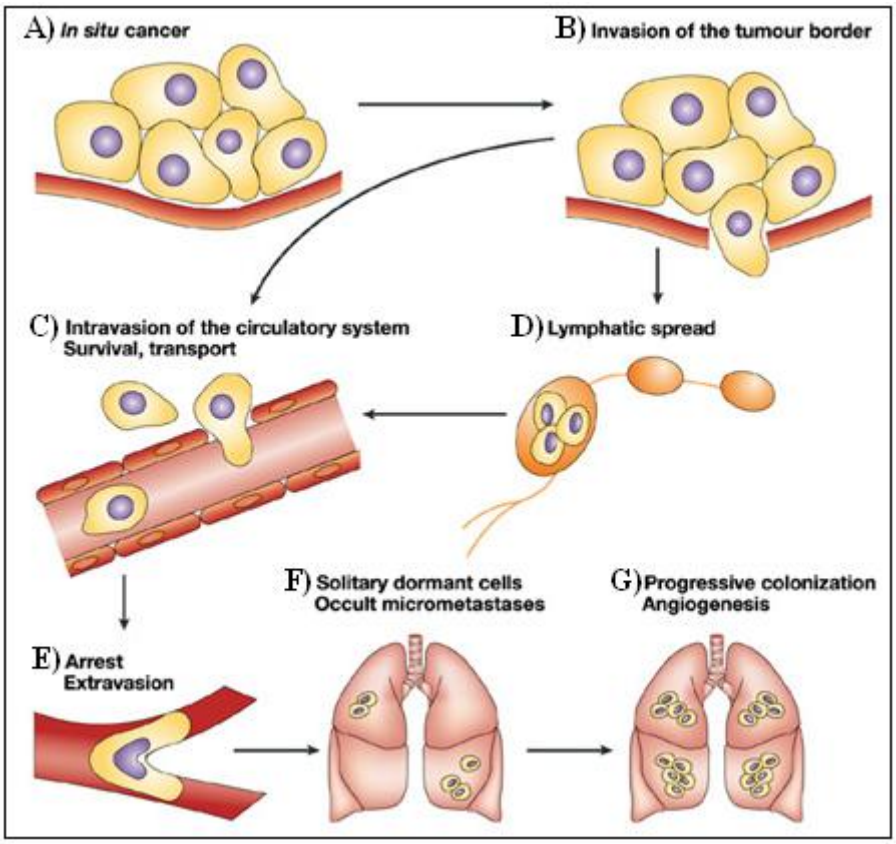

Figure 5. The metastatic cascade: A) *In situ* cancer must B) first invade the surrounding tissue and degrade the basement membrane. C) Next, cancer cells must intravasate to D) the vasculature or lymphatic system, and must both survive mechanic stress and evade immune destruction. E) Furthermore, the cancer cell has to arrest at a distant organ and extravasate. F) and G) in this hostile environment it has to proliferate and induce angiogenesis to colonize (adapted from (48)).

Two proposed models for the metastatic progression of solid tumors are the late dissemination model, also called the linear model, and the early disseminating model, also called the parallel progression model. In the late dissemination model the metastatic event is considered to occur late during tumor progression in the most advanced cancer cells in the tumor population (49). The idea is that the cells that disseminate escape from an established primary tumor. Indeed, for most tumors, the size is of prognostic value (50;51). This hypothesis is challenged by the early disseminating theory (49). In this model the ability of a cancer cell to metastasize is due to a genetic alteration established at an early time point in tumorgenesis in a subset of cells in the tumor population (52). This implies a genetic heterogeneity between the primary tumor and the metastatic lesion (51). Importantly, molecular profiling studies have shown data supporting both the late (53) and early (54) disseminating theories, and they are likely not mutually exclusive. Independent of

when the cancer cells disseminate from the primary tumor, there is a clear tendency for *where* they metastasize. For instance, breast cancer tend to metastasize to the bone, liver, lung and brain (55)**.** This property of metastasis as a non-random and organ specific process is not new, and was already presented by Stephen Paget in 1889 in the so called "Seed and soil" theory (56). Paget described metastasis as an interplay between the cancer cells, the "seed", and the specific organ microenvironment, the "soil" (56). The organ specific manner in which metastasis occurs may be explained by a permissive microenvironment at the distant site that supports the growth of the disseminating cells, for instance by secreted growth factors and supportive cells, in addition to intrinsic properties of the disseminating cell (43)**.**

Invasion is the first step in the metastatic process, and is one of the key features of malignant tumor cells. It is characterized by the loss of normal tissue constraints and cellular adhesion molecules, such as E-cadherin (57) This property of cancer cells resembles the tissue reorganization in early development: the epithelial to mesenchymal transition (EMT) (58), and the reactivation of EMT in cancer cells has been suggested as the mechanism by which they invade and metastasize (45)**.** EMT is a normal process in tissue growth and development, recognized by a loss of epithelial traits and the acquisition of mesenchymal cell markers**.** This transit is characterized by several reversible alterations, including change in cellular shape, increased motility, loss of apo-basal polarity and the down-regulation of adhesion molecules (45;59). In addition, the up-regulation of developmental transcription factors such as Slug, Snail and Twist has been linked to metastasis (58;60-62), supporting the link between EMT and metastasis. Another theory of the origin of the invasive properties of metastatic cells is the CSC theory. As previously described, this theory hypothesizes that only a subset of CSCs are capable of tumor propagation, thus implying that these cells must also be involved in the metastatic process. The rarity of CSCs in the tumor would also explain the inefficiency of metastasis, as only a few of the disseminating cells would have the capacity to colonize (1).

The final step of metastasis, colonization, relies on the ability to induce angiogenesis. Angiogenesis is the formation of new blood vessels from the preexisting vasculature, and is a normal process in growth and development as well as in wound healing and the reproductive cycle (1)**.** However, angiogenesis is also an important step in tumor

growth and in the process of metastasis (8). As the tumor reaches approximately 2-3 millimetres in diameter, oxygen, nutrients and elimination of waste by diffusion become insufficient, inducing a dormant tumor state (63;64). Thus, for further growth, the tumor mass is dependent on the infiltration of new blood vessels (65). Angiogenesis relies on the activation of vascular endothelial cells (65), which is regulated by a change in the balance between anti-angiogenic and pro-angiogenic signals, "the angiogenic switch" (8;66;67) (Figure 6). These signals include a range of growth factors such as vascular endothelial growth factor (VEGF), fibroblast growth factors and epidermal growth factors, which are secreted in the tumor microenvironment (65). In addition, hypoxia, the deprivation of oxygen, stimulates new vessel formation through the signaling of hypoxia-inducible transcription factors (HIFs) (66). The HIFs up-regulate many pro-angiogenic molecules such as VEGF, inducing a pro-angiogenic tumor microenvironment (65).

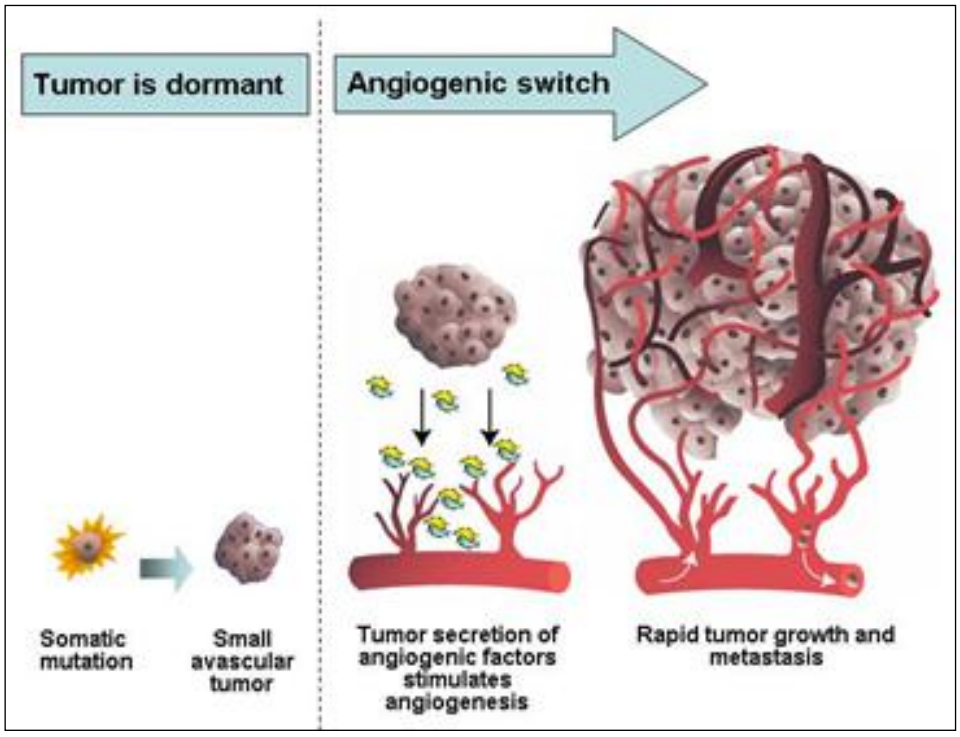

Figure 6. The angiogenic switch. Tumor development is initially restrained by a lack of nutrition and oxygen. Further growth requires vascularization of the tumor, the process of angiogenesis. Importantly, the infiltrating blood vessels also provide a direct route for both primary and metastatic lesions to further metastasize (modified from (68)).

1.5 Signal transduction in breast cancer

The transduction of extracellular signals to an intracellular response is an essential property of multicellular organisms in order to regulate normal tissue growth and homeostasis (1). The binding of an extracellular ligand, for instance a growth factor, to a receptor on the cell membrane, leads to activation through phosphorylation of the intracellular domain (69). This signal is transmitted by a cascade of phosphorylations of downstream targets, and is ultimately propagated to the nucleus where it activates transcription factors involved in the regulation of cell proliferation, differentiation and survival**.** In cancer cells, many signaling pathways are frequently deregulated (70), which has led to the development of pathway-targeted therapy that inhibit specific molecules in signaling pathways.

The phospatidylinositol-3-phosphate kinase (PI3K)/Akt pathway is frequently activated in human cancers, including breast cancer, by amplification, mutation or translocation of one of numerous components in the signaling network (71-73). Most commonly this is due to an inactivating loss-of-function mutation in the gene encoding the tumor suppressor phosphatase and tensin homologue (PTEN), or by an activating gain-of-function mutation in the *PIK3CA* gene, encoding the catalytic subunit of PI3K (71;74;75)**.** The pathway is central in many cellular processes implicated in cancer such as cell growth, cell cycle progression, glucose metabolism, migration, EMT, angiogenesis and cell survival (76;77).

An overview over this complex pathway is illustrated in Figure 7. The PI3K/Akt pathway is activated upon binding of a ligand, such as a growth factor, to a receptor tyrosine kinase (RTK) on the cell membrane, with the subsequent activation of its intracellular domain (76;78). This creates a docking site for the recruitment and activation of the PI3K which subsequently converts phosphatidylinositol-3,4-biphosphate (PIP_2) to phosphatidylinositol-3,4,5 triphosphate (PIP_3). PIP_3 has a dual role in activating Akt: it activates phosphoinositide dependent kinase 1 (PDK1) and recruits Akt to the plasma membrane (79). Here, Akt is activated by PDK1 mediated phosphorylation on Thr308 (73;78;80;81). The phosphorylation of Akt at Ser473 is required for its full activation and many enzyme candidates have been suggested for this modification, including the mammalian target of Rapamycin 2 (mTOR2)

(73;79;82). The pathway is negatively regulated by PTEN, whose action reverses the PIP_2-PIP_3 transition, and thus impedes the activation of Akt (83). The PI3K/Akt signaling pathway regulates a network of signaling cascades, for instance the mTOR1 pathway, which induces cell growth through activation of p70S6K, and inhibition of 4EBP1, which promotes protein synthesis. Activated mTOR1 is central in regulating cell growth and homeostasis, and is commonly implicated in cancer (84). Furthermore, the PI3K/Akt pathway has been demonstrated to be involved in chemoresistance in ovarian and breast cancer (85;86). The PI3K/Akt signaling network therefore represents a promising target for cancer drug discoveries either by preferentially killing cancer cells or sensitizing them to conventional chemoterapeutics (71;86).

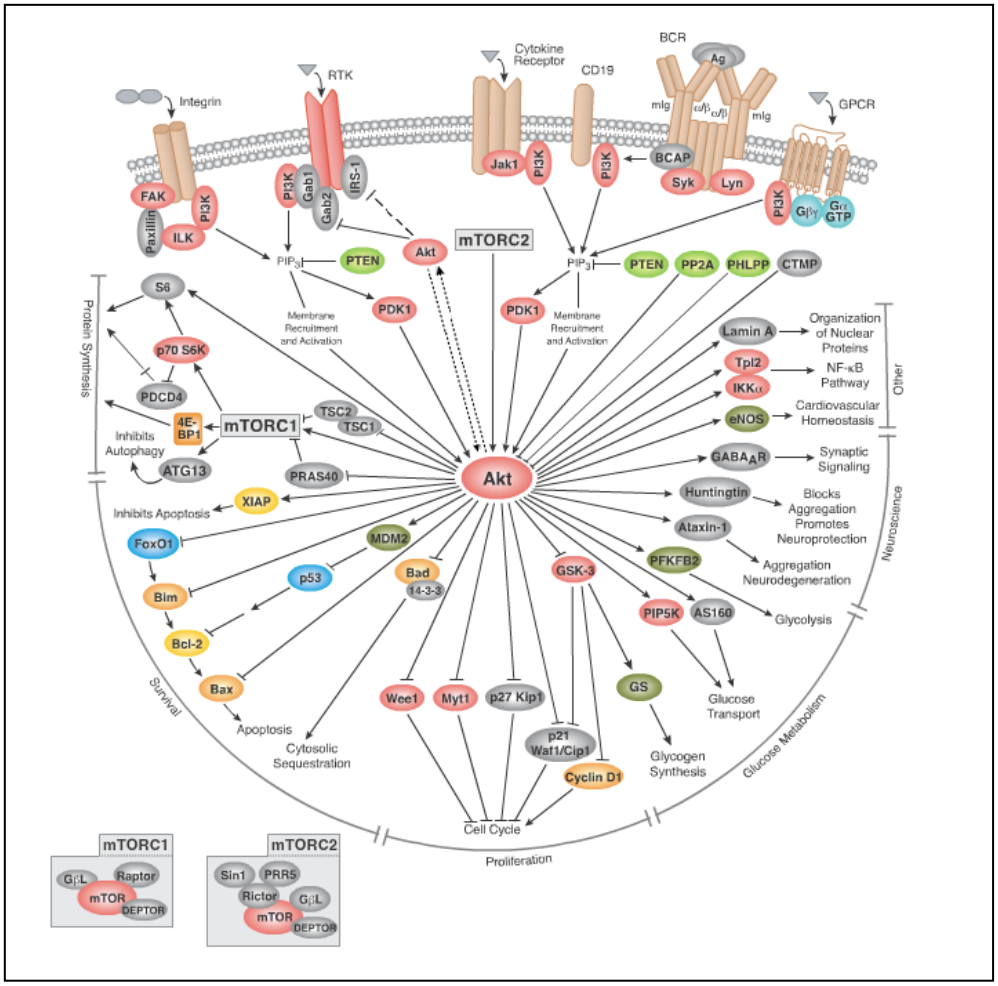

Figure 7. The PI3K/Akt pathway regulates many cellular properties. The pathway transduces extracellular signals such as integrins, cytokines and growth factors from the cell membrane to the nucleus through the phosphorylation of numerous proteins (76;78). Akt kinase is at a nodal point in this network (available from (87)).

1.6 Resistance to anti-cancer drugs

Chemotherapy represents a major therapeutic management of breast cancer, and a major challenge of systemic treatment is the emerging resistance by tumors, in particular by metastatic disease, to treatment.

Chemoresistance may be an intrinsic property of the cancer cell, or it may develop during treatment. A property of acquired resistance is that it frequently induces a broader resistance to other drugs with different mechanisms of action, rendering the metastatic cells multi-drug resistant (38). There are many factors involved in chemoresistance, and both the limitations of drugs reaching the center of the tumor and the tumor micro-environment, contribute to the lack of effect of systemic treatment. In addition, there are several cancer cell specific resistance mechanisms such as increased drug efflux, decreased drug influx, drug inactivation, alterations in drug target, processing of drug-induced damage and evasion of apoptosis. These cellular properties of chemoresistance are illustrated in Figure 8 (38).

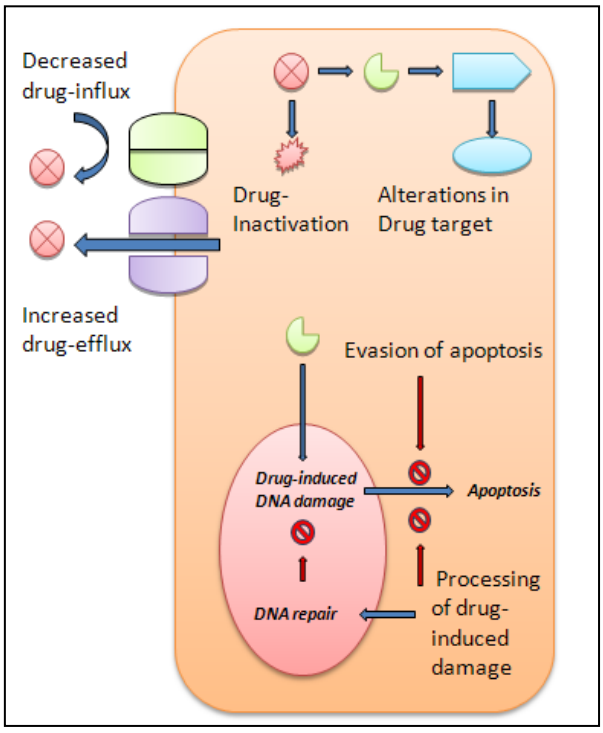

Figure 8. The cancer cell specific mechanisms of resistance to chemotherapy and anti-cancer drugs; decreased drug influx, increased drug efflux, increased drug inactivation, alterations in the drug target, antagonizing drug-induced damage, here illustrated by an increased DNA-repair and evasion of apoptosis (38).

The growing understanding of cancer cell biology has led to the emerging field of targeted therapy, which aims to kill cancer cells specifically, by targeting molecular mechanisms that are critical for the cancer cells' growth and survival. However, many of the cellular mechanisms involved in chemoresistance are also able to render the tumor cells resistant to small molecule inhibitors. In addition, an extensive crosstalk between multiple pathways in the cell may counteract the effect of small molecule inhibitors by compensatory mechanisms. Clearly, understanding the molecular mechanisms that influence response has great therapeutic value. This would allow rational combinations of different anti-cancer therapies, where targeted agents can be used in combination with other anti-cancer drugs to increase their efficacy (38).

1.7 The B7-H3 protein, a member of the B7/CD28 family of co-stimulatory proteins

B7-H3 (CD276) is a member of the B7 family of co-stimulatory ligands. A high expression of this protein has been associated with advanced disease and poor prognosis in several tumor forms, including breast cancer (88;89). B7-H3 is the focus in the present thesis, and will thus be further described in this section.

The B7 family consists of 7 members of immunoregulatory ligands (B7-1, B7-2, B7-H2, B7-H1, B7-DC, B7-H3 and B7-H4) which display both inhibitory and stimulatory effects with regard to T cell activation (90). Each ligand and their corresponding receptor are schematically illustrated in Figure 9.

The activation of a T cell depends on its interaction with an antigen, in addition to costimulatory signals delivered by the B7 family of ligands through cognate receptors on the T cell membrane. The B7 family are transmembrane proteins (with the exception of B7-H4), that show a high degree of structural conservation. They have an immunoglobulin variable (IgV)-like and an immunoglobulin constant (IgC)-like domain in their extracellular region, a transmembrane region and a cytoplasmic tail (91).

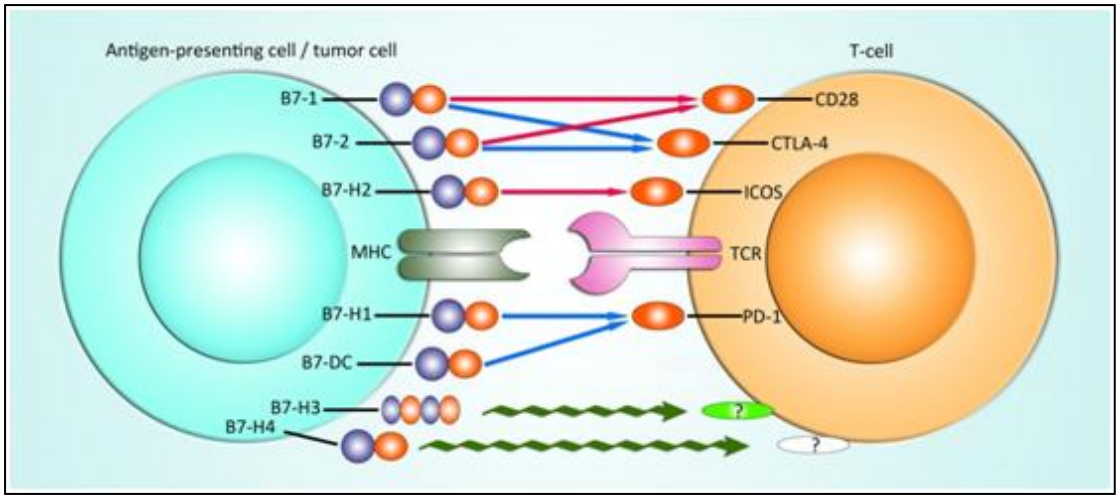

Figure 9: An overview of the B7 family of immunoregulatory ligands. The T cell is activated through interaction with the MHC complex and an antigen on an antigen-presenting cell, in addition to an integration of signaling through the B7 familiy of co-stimulatory receptors.

The B7-H3 protein was identified as a member of the B7 family in 2001 (92). It consists of 534 amino acids and has a molecular weight of approximately 100 kDa. The high molecular weight is attributed to the fact that the protein is highly glycosylated (93). The ligand exists in two different isoforms: the 2IgB7-H3 and the 4IgB7-H3, with the latter containing two constant and two variable domains, and is the dominant isoform expressed in human tissues (90). The expression of B7-H3 is inducible on antigen presenting cells, T cells and natural killer cells (88). In addition, the protein is expressed on cells within non-lymphoid organs and at a high expression level in a variety of cancer types (88).

Initially, the expression of B7-H3 was shown to correlate with T-cell activation and IFN-gamma production (92). However, contrasting studies have showed both stimulatory and inhibitory effects of B7-H3 on T-cell response and anti-tumor activity (92;94-96). Moreover, multiple studies have correlated a high B7-H3 expression with disease spread and poor outcome in different cancer types (89;97;98).

The conflicting roles of B7-H3 may be explained by several factors. The cognate receptors have not been identified. Although the triggering receptor expressed on myeloid cells-like receptor 2 (TLT-2) has been suggested as the receptor for B7-H3 (99), this was not confirmed by physical interaction studies performed by Leitner *et al* (94). The identification of its receptor(s) could help unravel the contrasting role of

B7-H3 in immune response. However, it is likely that B7-H3 might interact with several proteins, accounting for its diverse functions in different tumors. The expression patterns of these receptor(s) may also influence the immune modularly role exerted by B7-H3. In addition, several studies on B7-H3 are based on mouse models, and there are uncertainties with regard to whether these effects can be extrapolated to humans (88).

Although most studies on the adverse effects of high B7-H3 expression in cancer is related to its immunoregulatory role, recent studies have identified novel non-immunological function of B7-H3 in metastasis and chemoresistance. A high B7-H3 expression has been associated with increased tumor cell migration and invasion *in vitro* and *in vivo*, thus contributing to the metastatic capacity of cancer cells (100;101). Another study showed that B7-H3 expression was involved in Paclitaxel resistance in B7-H3 expressing breast cancer cell lines both *in vitro* and *in vivo* (102). It remains to identify the exact physiological role of B7-H3 in normal tissue, and cancer. However, its implications in malignant processes and the elevated expression on a wide range of tumor forms make it a putative prognostic and possibly therapeutic target.

2. Material and methods

All methods used in this thesis are described below, the reagents and equipments utilized are listed in Appendix A.

2.1 Breast cancer cell lines

Two breast cancer cell lines, MDA-MB-435 and MDA-MB-231, were used in this thesis. The cell lines were originally purchased from the American Type Culture Collection. Both cell lines are triple negative (ER-, PR- and HER2-) metastatic breast cancer cell lines with a high expression of the B7-H3 protein. B7-H3 silenced models of these cell lines have previously been established using stable short hairpin (sh) RNA with HuSH 29mer short hairpin RNA (shRNA) constructs against B7-H3 (shB7-H3) and control plasmid pRS nontargeted TR30003 (TR33) (Origene Technologies, Inc, USA). Selection with 0.5 mg/µl puromycin was used to isolate successful clones (102). Cells with B7-H3 knockdown are referred to as shB7-H3 and their vector control counterparts are referred to as TR33 in this thesis. The TR33 cells contain a non-targeting RNA sequence and express the B7-H3 protein. This model system, with the MDA-MB-435 and MDA-MB-231 cell variants TR33 and shB7-H3, allowed the investigation of the possible involvement of B7-H3 in resistance to anti-cancer drugs and the investigation of molecular mechanisms behind any putative different efficacy.

2.2 Cell culturing

Cell culturing was performed in sterile conditions in a laminar flow hood (LFH), which was disinfected with 75 % ethanol prior to use to prevent infections. Only one cell line was kept in the LFH at the time, and the LFH was disinfected between working with different cell lines. Gloves were used at all times, and all equipments were disinfected with 75 % ethanol before entering the LFH. Growth medium was heated to 37^0C prior to use. In addition, all cells where grown on tissue-culture treated 100x20 mm Corning Petri dishes (Corning Incorporated, NY USA). The cell lines were maintained in Dulbecco's Modified Eagle's Medium (DMEM) (4,5 g/l glucose,

without L-Glutamine, SIGMA-ALDRICH®, USA) supplemented with 10 mM 4-(2-hydroxyethyl)-1-piperazineethanesulfonic acid (HEPES) (Invitrogen, Life Technologies™, USA), 10% fetal bovine serum (FBS) (GIBCO®, Life Technologies™, USA), 5mL GlutaMAX (GIBCO®, Life Technologies™, USA), Penicilin and Streptomycin (5mL, 5000 U pen/mL, 5000 U strep/mL) (GIBCO®, Life Technologies™, USA) and 0.5µg/mL puromycin (10mg/mL, SIGMA-ALDRICH®, USA) and incubated in NuAire Automatic CO_2 incubator (NuAire, USA) at 37^0C with 5% CO_2**.**

Cells were obtained from a liquid nitrogen tank where they had been stored at -170^0 C in a solution containing growth medium and 5 % Dimethyl Sulfoxide (DMSO) (Thermo Scientific, USA). DMSO is a cryopreservant and may be harmful to cells at room temperature, and the transfer to fresh medium and subsequent centrifugation was performed quickly to prevent toxic effects of DMSO on the cells. The cell pellets were transferred to 15 mL Sarstedt tubes (Sarstedt, USA) containing 8mL growth medium, following centrifugation at 800 rpm for 8 min in a Rotina 420 centrifuge (Hettichlab, Germany). The supernatant was discarded and the cell pellet resuspended in growth medium and plated on Corning Petri dishes and incubated at 37^0C with 5% CO_2 saturation. All cells were grown for 2 weeks prior to conduction of experiments to ensure that they were stable and not damaged by the freezing or thawing.

Renewal of medium was performed by discarding old medium and adding 10 mL of fresh medium to the Petri Dish. Cell lines, when they reached a confluence level of approximately 80% as observed by an Axiovert 40 inverted microscope (Carl Zeiss, Germany), were split by discarding old medium, and subsequently washing the Petri dish with 3 mL Dulbecco's Phosphate buffered Saline (DPBS) (1X, Invitrogen, Life Technologies™, USA) to remove remaining medium. The cells were detached from the Petri dish by adding 1.5 mL 0.25 % Trypsin EDTA (GIBCO®, Life Technologies™, USA) for 4 minutes at 37^0C. The medium contains divalent ions, such as Mg^{2+} and Ca^{2+}, in addition to proteins that inhibit Trypsin. By washing with PBS, the remains of the medium were removed. The EDTA supplemented in the Trypsin solution is also a chelator that binds remaining ions. When the cells were detached from the Petri dish, as observed in the Axiovert 40 inverted microscope, growth medium was added to inhibit Trypsin activity. The cells were subsequently

transferred to 15 mL Sarstedt tubes and centrifuged at 800 rpm for 8 minutes. The supernatant was discarded and the cell pellet resuspended in growth medium and diluted to obtain the appropriate sub-culturing ratio. The cells were replated on new Petri dishes containing 10 mL growth medium and incubated at 37^0C and 5% CO_2 saturation.

2.3 Cell counting using hemocytometer

The cells were counted using a Bürker hemocytometer in both the optimizing procedure and the drug screening procedure. The hemocytometer and the cover slip were cleaned by washing with 75 % ethanol and then rinsed with distilled water. Cells were detached from the Petri dish by trypsinating and spun down as described above. The old medium was discarded, and the cell pellet resuspended in 8-10 mL growth medium. As any groups of cells that are attached together are counted as one, it was important that the cells were thoroughly suspended in order to achieve an accurate count. 10µl of the cell suspension was then carefully applied to a Bürker chamber and covered with a cover-slip. Five of the squares were utilized for counting, and an average of these was used to calculate the number of cells in the suspension. To achieve a representative count it was important that each square contained between 40-100 cells and that there was a low variance between the counted squares. The volume suspension in one square equals 0.1 µl and the total amount of cells per mL in the suspension was thus the average cell count x 10 000.

2.4 The Cell titer glo® (CTG) Luminescent cell viability assay

The CTG luminescent cell viability assay (Promega, USA) was used as an endpoint of the optimizing and drug screening procedures as a quantitative method to determine the number of metabolically active cells. The CTG reagent has two distinct properties; it causes cell lysis and thus the release of ATP from the cells. The ATP converts Luciferin to Oxyluciferin and a luminescent light, catalyzed by the Luciferase enzyme, as illustrated in Figure 10. The amount of luminescence is directly

proportional to the amount of ATP in the cells, and thus gives a quantitative measurement of cell viability (103).

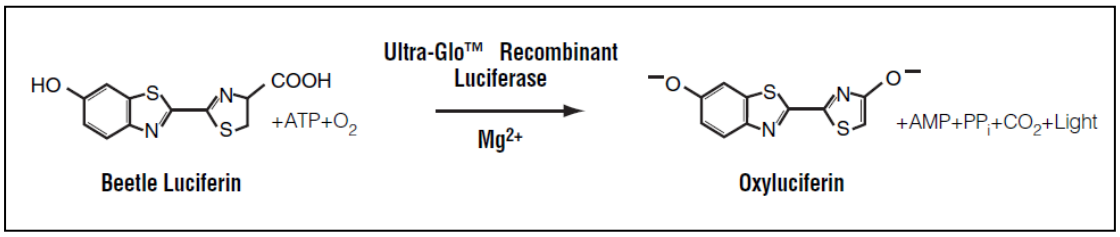

Figure 10. The luciferase reaction. Lucuferin is converted to Oxyluciferin and luminescence in the presence of ATP, cellular oxygen and the cofactor Mg^{2+}. The amount of luminescence produced is directly proportional to the amount of ATP in the cells (103).

2.5 Optimizing of cell lines for growth in 384 well plates

In order to achieve the optimal cell number to apply to each well in the drug screening, the cells were optimized for growth in 384 well plates (Greiner bio-one, North-America). The cell lines MDA-MB-435 (TR33 and shB7-H3) and MDA-MB-231 (TR33 and shB7-H3) were seeded in the 384 well plates at different dilutions, ranging from 300 to 1200 cells per well, depending on the proliferative rate of the cell lines. 50 µl of each dilution was applied to the 384 well plates in seven replicas. The outer wells were avoided due to an increased risk of evaporation. The plates were subsequently placed in open zip-lock bags with a moist tissue (dH_2O) in the opening of the bag to avoid evaporation of nutrient medium, and then incubated for five days at 37^0C and 5% CO_2 saturation. At day five the cells were lysed by adding 20 µl CTG to each well, and incubating at room temperature for 35 minutes. The plates were covered with aluminum foil, as the assay is light sensitive. Luminescence was measured using Wallac 1450 MicroBeta TriLux luminescence counter (PerkinElmer, USA) with the MicroBeta Windows Workstation (PerkinElmer, USA). The MicroBeta Trilux is a multi-detector instrument designed for the detection of luminescence in microplates. The counter has two detectors that register luminescence from the top to the middle of the plate, and from the middle to the bottom of the plate. Reliable results were assured by calculating standard deviations of all measurements. The results were analyzed by making growth curves in Microsoft Office Excel (2007).

The cell numbers where the cells appeared to be in logarithmic growth phase were chosen for drug screening.

2.6 Drug screening of B7-H3 expressing and B7-H3 silenced breast cancer cell lines

2.6.1 Description of the drugs screened and plate annotation.

A panel of 22 different anti-cancer compounds targeting receptor tyrosine kinases and their downstream pathways was used in the drug screening, in addition to drugs targeting the estrogen receptor (4-Hydroxytamoxifen), protein complexes, and enzymes: topoisomerase II (Bortezomib), proteasome (Doxorubicin hydrochloride) and the Heat Shock Protein 90 (HSP90) (Radicicol). Drugs and their targets in the cell, including their concentrations, are presented in Table 1. The drug plates were not commercially available but were provided frozen in sealed 384 well plates by our collaborator, Medical Biotechnology, VTT Technical Research Center of Finland. The different compounds had been printed onto a 384 well plate with the Hamilton Microlab Star Robot (Hamilton Robotics, Switxerland). Each drug was printed in duplicate on the plate at seven dilutions with 10 times increment in concentration from the middle of the plate to the border, as illustrated in Figure 11. The edges of the plates were filled with DMSO and thus not utilized for the screening procedure due to the risk of evaporation from the outer wells. Drug screening was performed twice for each cell line at separate days, and with cell numbers obtained from the optimizing procedure.

Table 1: The panel of 22 drugs used in the drug screening. The target site of the drug is noted, together with the lowest and the highest concentration of the drug printed to the plates.

Site	Number on plate	Compound	Lowest concentration (pM)	Highest concentration (µM)
HER2	22	Herceptin	5	5
	17	Symansis CP-724714	20	20
EGFR	18	Gefitinib	20	20
	14	PD153035 hydrochloride	20	20
EGFR + HER2	5	BIBW2992	20	20
	15	Lapatinib (GW572016)	20	20
pan-ErbB	11	CI-1033	20	20
PI3K + mTOR1	8	PI 103 hydrochloride	20	20
PI3K	13	Wortmannin	20	20
Hsp90	2	Radicicol	20	20
AKT/PKB	1	Akt1/2 kinase inhibitor	20	20
	6	API-2	20	20
mTOR1	12	Everolimus	20	20
	19	Temsirolimus	20	20
MEK/ERK	4	PD 184352	8	8
	9	UO126	20	20
ER	20	4-hydroxytamoxifen	20	20
Proteasome	16	Bortezomib	5.2	5.2
Topo2	10	doxorubicin hydrochloride	20	20
IGFR	3	AG 538	20	20
VEGFR	7	AAL-993	20	20
	21	Bevacizumab	0.34	0.34

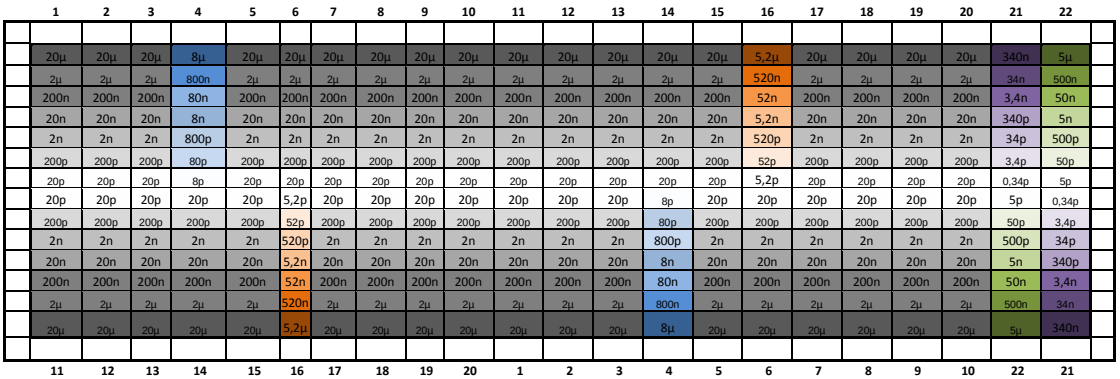

Figure 11. Plate design for the drug screening. Drugs were printed in two replicates with increasing concentration starting from the middle of the plate (light colors) towards the edge (dark colours). The different dilutions ranging from 20 pM to 20 µM except blue; 8 pM - 8 µM, orange; 52 pM - 5.2 µM, green; 5 pM – 5 µM and purple; 0.34 pM – 340 nM. The numbers at the borders represent the drugs in the location, and are presented in Table 1. The outer wells contained DMSO.

2.6.2 The drug screening procedure in 384 well plates

All cells were healthy and had reached a confluence level of approximately 80 % before they were applied to the drug screening assay. The handling of the drug plate was done according to the health and safety procedure of the lab: A special LFH was utilized and nitrile gloves were worn at all times, and the plates were kept in the LFH at all times between handling. The LFH was covered with Versi-Dry Lab-Soakers (Nalgene, Thermo Scientific, USA) and the plate and all equipments were kept on this sheet at all times. All areas that had been in contact with the drug plate were washed with ethanol. Furthermore, all equipments, gloves and the drug plates were placed in a zip-lock bag and disposed of in an appropriate container for cytostatic waste after use, according to the health and safety procedures in the laboratory.

The drug screening plate was thawed at room temperature for 30 minutes prior to use, and then centrifuged for 1 minute at 1000 rpm to spin down the drugs. The optimum cell number obtained from the optimization procedure was prepared by counting with a hemocytometer as described previously. The plates were unsealed using a Combi Thermo sealer (ABgene, UK), and 50 µl cell suspension was dispensed to each well by a Multidrop Reagent dispenser Combi (Thermo Fischer Scientific, USA) (Adjustments: 384 well plate standard, 15 mm, 50 µl standard tube cassette, speed: low). The reagent dispenser was washed with distilled water (GIBCO®, Life Technologies™, USA), ethanol (75%) and distilled water before and after use. In addition, initial priming with cell suspension was done to control the flow in all eight tubes. By applying the cell suspension with a reagent dispenser, error due to manual pipetting was reduced. The 384 well drug plate was subsequently placed in an open zip-lock bag with a moist tissue to prevent dehydration and incubated for five days at 37^0C and 5% CO_2 saturation. At day five the plates were placed in the LFH for 30 minutes to reach room temperature before adding 20 µl CTG by the reagent dispenser (Adjustments; 384 standard, 15 mm, 20 µl standard tube cassette, speed low). The plate was covered with aluminium foil to protect the CTG from light exposure and then incubated for 35 minutes in the LFH. After incubation with CTG, the drug plate was transported to the luminescence counter in a Nalgene Bio Transport Carrier (Nalgene, NY, USA) designed to transport potentially hazardous material, to a Wallac

luminescence counter where the luminescence was measured. The workflow of the drug screening assay is illustrated in Figure 12.

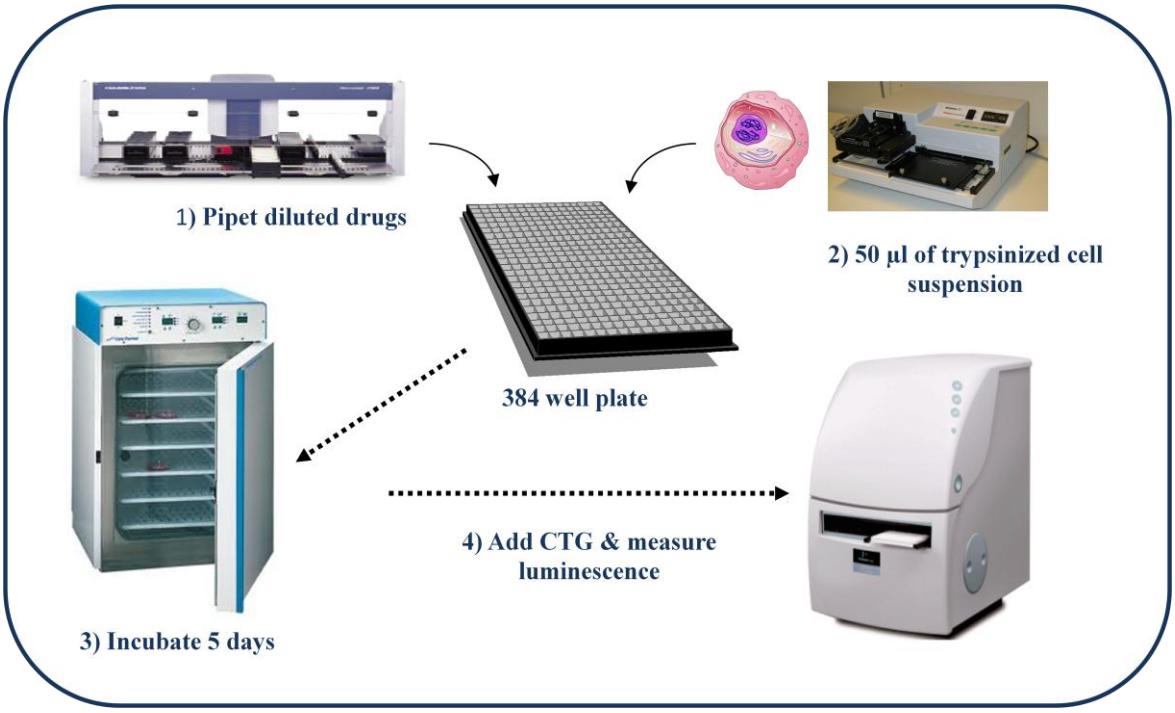

Figure 12. The workflow of drug screening procedure in 384 well plates. The drugs were printed onto 384 well plates, and the cell suspension was added using a Multidrop Combi (Thermo Fischer Scientific, Finland). The plates were subsequently incubated for five days at 37°C with 5 % CO_2. At day five the cells were lysed with the Cell Titer-Glo (CTG) luminescent Cell Viability Assay. CTG measures ATP in the cells, and thus gives a quantitative measurement of cell viability.

2.7 Statistical analyses and growth inhibition curves

To investigate the effect of B7-H3 knockdown on drug response the drug efficacy was evaluated by comparing the response of B7-H3 knockdown cells to their B7-H3 expressing counterparts (*i.e.* MDA-MB-435 shB7-H3 compared to TR33, MDA-MB-231 shB7-H3 compared to TR33). All data was normalized to cells growing at the lowest drug concentration before any statistical analysis was calculated, and the normalized data is referred to as the relative response. Hence, the measurement at the lowest concentrations was excluded from further analysis. Statistical significance was assessed by performing a two-tailed Student's (Excel, Microsoft Office Excel (2007), Seattle, WA, USA). This test evaluates the differences in means of two datasets. The

test calculates a p-value, which is the probability of obtaining a test statistic (a difference in means) as extreme as the one observed given that there is no difference. A low p-value thus implies a low probability of obtaining the given results by random chance and all p-values below 0.05 were considered statistically significant. The growth inhibition curves were made by plotting the relative response versus the drug concentration using the Graphpad prism software (Graphpad Prism Software Inc., USA). The curves were log transformed, and EC_{50} values calculated from curves that followed a sigmoid curve (S-shaped).

2.8 Treatment of MDA-MB-231 and MDA-MB-435 cell variants with API-2 and Everolimus

To further investigate the molecular mechanisms behind the differences in drug response to selected drugs, Western blot analysis was performed on protein targets in the pathway affected by the small molecule inhibitors. MDA-MB-231 and MDA-MB-435 cell variants, TR33 and shB7-H3, were investigated with respect to differences in the activity levels of proteins at different time points after treatment. Cells were plated at appropriate cell number and treated the subsequent day with drug concentrations obtained from the drug screening assay. MDA-MB-435, TR33 and shB7-H3, were treated with API-2 (20 µM) (SIGMA-ALDRICH®, USA) and harvested at time: 0 hours (no treatment), 0.5 hours and 2 hours. MDA-MB-231, TR33 and shB7-H3, were treated with API-2 (2 µM**)** and harvested at time: 0 hours (no treatment), 0.5 hours and 2 hours. MDA-MB-231, TR33 and shB7-H3, were in addition treated with Everolimus (200 nM) (SIGMA-ALDRICH®, USA) and harvested at time: 0 hours (no treatment), 0.5 hours and 2.

2.9 Harvesting of cells

The old medium was discarded and the cell culture flask placed on ice. 3 mL cold PBS supplemented with phospho-STOP Phosphatase inhibitor cocktail tablets (Roche, Germany) was added to the flask and the cells were detached by gently scraping the base of the flask with a cell scrape (TPP Techno Plastic Products AG, Switzerland). The cell suspension was transferred to a 50 mL Sarstedt tube and centrifuged in a

Heraus Labofuge 400R (Thermo scientific, USA) at 1200 rcf for 5 minutes at 4^0C. The supernatant was discarded, and the cell pellet washed by resuspending in 1 mL phospho-STOP supplementet PBS and transferred to 1.5 mL eppendorf tubes. The samples were subsequently centrifuged in a Spectrafuge^{TM} 24D Digital Microsentrifuge (Labnet international, USA) at 14 000 rpm for 5 minutes at 4^0C, the supernatant were discarded and the dry pellets subsequently stored in a freezer at -80 ^{0}C or directly lysed.

2.10 Cell lysis

The cells were lysed to obtain their protein contents. In this thesis, protein activity levels were measured with regard to phosphorylated proteins. Protein modification by phosphorylation leads to their activation or inactivation, and is a dynamic and transient alteration regulating protein activity in many cellular processes. The phosphate group can thus easily be removed by phosphatases intrinsically present in the cells. To maintain the proteins in their phosphorylated state and prevent potential degradation of proteins, the lysis buffer (LB) (Appendix B) was supplemented with broad spectrum inhibitors of phosphatises and proteases that are endogenous present in the cell lysate. In addition, the LB also contained an appropriate buffer solution and substances that disintegrated the cytoplasmic membranes of the cells' compartments. The cells were lysed with LB, and the amount used was dependent on the size of the cell pellets (varied between 10-50µl), and subsequently placed on ice for 20 minutes. The samples were then sonicated using an Ultrasonic homogenizer (Cole-Parmer 4710 series, Chicago, USA) three times for five seconds at 4^0C, and incubated at -80^0C for 5 minutes. The sonication and the freezing further disintegrated the cell membranes and other cellular structures mechanically, and released the protein contents of the cells. Further, the cell pellets were centrifuged for 15 minutes at 14 000 rpm and 4^0C in a Microcentrifuge. The supernatant was retained and protein concentrations measured by the BCA assay.

2.11 Measuring protein concentrations by the BCA assay

The Pierce® BCA Protein Assay Kit (Thermo Scientific, USA) was utilized to measure protein concentrations in the cell lysate. This is a quantitative method to determine protein concentration based on the Biuret reaction and the reaction of cuprous ions with Bicinchoninic acid (BCA). The BSA standards were prepared according to the protocol provided by the manufacturer and are attached in Appendix B (104).

Samples and LB (blank test) were diluted 20 times (3 µl sample/LB solution + 57 µl dH_2O). Subsequently, 25 µl of each Bovnie serum albumin standard dilution (A-F), sample and blank were pipetted in duplicate on a Corning® Costar® 96 well cell culture plate (Corning Incorporated, SIGMA-ALDRICH, USA). The working reagent (WR) was prepared by mixing 50 parts of BCA Reagent A (containing an alkaline environment, BCA and Sodium Tartrate) with one part of BCA reagent B (containing 4 % cupric sulphate). 200µl of WR was added to each well followed by 30 minutes incubation at 37 ^{0}C in a Termaks drying oven (Termaks, VWR, USA). This provided the appropriate conditions for the biuret reaction where Cu^{2+} first chelates with peptides containing three or more amino acid residues in an alkaline environment, a reaction that results in the reduction from cupric to cuprous ions. Secondly, the BCA forms a deep purple colour complex with Cu^{+1}. This complex is water-soluble and its colour intensity is directly proportional to the protein concentration in the solution (105). The reaction exhibits a strong linear absorbance at 568nm with increasing protein concentration within a working range of 20-2.000µg/mL (104). The absorbance was measured with the Wallac Victor^2 1420 Multilabel Counter (PerkinElmer, USA) with the Wallac 1420 workstation at 540 nm, and the averages of the blank standard replicates were subtracted from all measurements. The correct calculation of protein concentration was based on a standard curve prepared in Microsoft Office Excel (2007) by plotting measured blank-corrected BSA standard absorbencies to their concentration (µg/mL). The concentrations of the samples were calculated by means of the equation of the linear regression ($y = ax + b$) to this curve.

2.12 Western blot

The Western blot procedure separates proteins based on their size as they migrate through a polyacrylamide gel, and subsequently transfer the proteins to a membrane where they can be stained by antibodies for protein detection. An overview of the entire procedure is presented in Figure 13.

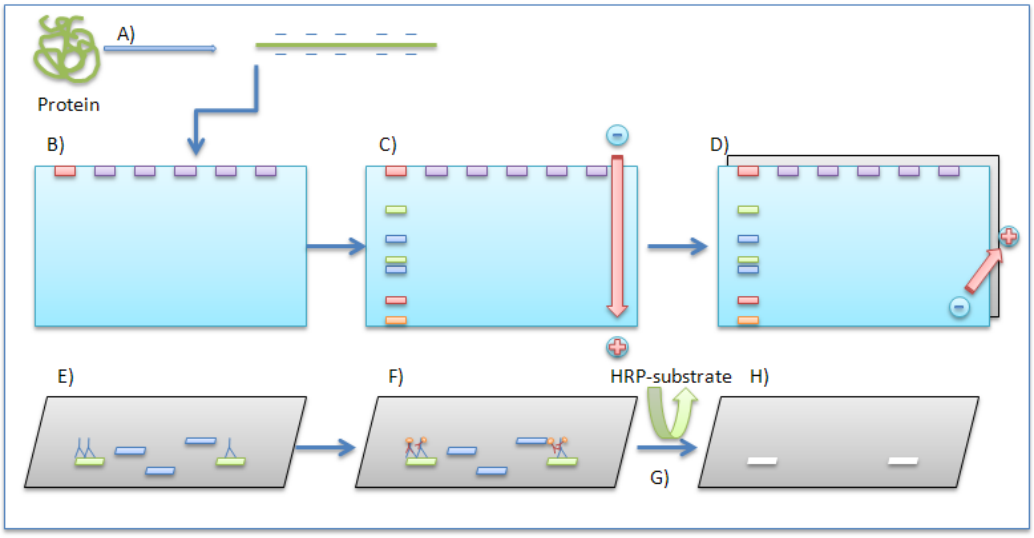

Figure 13. The outline of the Western blot procedure: A) the protein is linearized and gets a net negative charge by adding SDS and heat, B) samples are loaded to a gel, a ladder (size marker) is added to well one, C) an electric current is applied to the gel and smaller proteins will migrate fast than larger proteins through the gel network, enabling the protein separation based on size, D) proteins are electrotransferred to a PVDF membrane, E) the membrane is blocked to avoid unspecific binding, and primary antibody specific for the relevant protein (green) is added, F) secondary HRP-coupled protein is added, which recognize and bind to the primary antibody, G) HRP-substrate is added and H) The luminescent light is detected in a imaging machine.

The procedure can be divided into several steps described underneath.

Step 1: Preparation of protein samples for loading on the gel and separation by SDS-PAGE

The protein lysates were kept on ice while preparing the samples. The required sample volume was calculated from the BSA assay to achieve a final protein loading concentration of 20µg. 2µl NuPage® Sample Reducing agent (10x) (RA) (Life Technologies™, USA) and 5µl NuPage® LDS Sample Buffer (4x) (LB) (Invitrogen™, Technologies™, USA) were added to the protein samples and

supplemented with dH_2O to reach a final sample volume of 20 µl. Subsequently, the proteins were denatured by incubating the samples on a Grant Dry Block Heater (QBD2) (Grant, USA) for 5 minutes at 95 ^{0}C, and then quickly centrifuged in a Micro120 Centrifuge (Hettich, Germany) for 1 min, at 12 000 rpm. In these steps, a net reduction of the proteins in the samples was obtained by adding the RA, thus breaking the cystein bonds in the proteins. Subsequent heating further denaturized the proteins, ensuring that they were in a linear form. This enabled the separation of the proteins according to size when migrating through the network of the gel (Figure 13 A). The LB contains glycerol, ensuring that each sample sinks to the bottom of the well when applied onto the gel. A NuPage® Bis-Tris (4-12%, 0.1mm x 10 well, Life Technologies™, USA) polyacrylamid gel was mounted in an XCell SureLock™ Mini-Cell (Life Technologies™, USA). The inner concealed compartment and the surrounding compartment were filled with Running Buffer consisting of 50 mL NuPage® MES SDS Running Buffer (20x) (Life Technologies™, USA and 950 mL dH_2O. 10 µl SeeBlue®Plus2 Prestained Standard (1x) (Invitrogen, Life Technologies™, USA) was used as a molecular weight reference, and 20µl of each sample was loaded onto the gel. An overview over mounting of the electrophoresis chamber is illustrated in Figure 14. Electricity was applied to the system using a Power Pac 300 (BioRad, USA) at 105 V. This separated the negatively charged proteins as they migrated towards the positive pole. The velocity at which the proteins travel was dependent on their size, with smaller proteins migrating faster (Figure 13.B and C). When applying electricity, bubbles from the bottom of the inner chamber confirmed that the system was working. After 10 minutes the voltage was adjusted to 150 V, and the gel was run for approximately 1.5 hours, depending on the protein targeted for the separation.

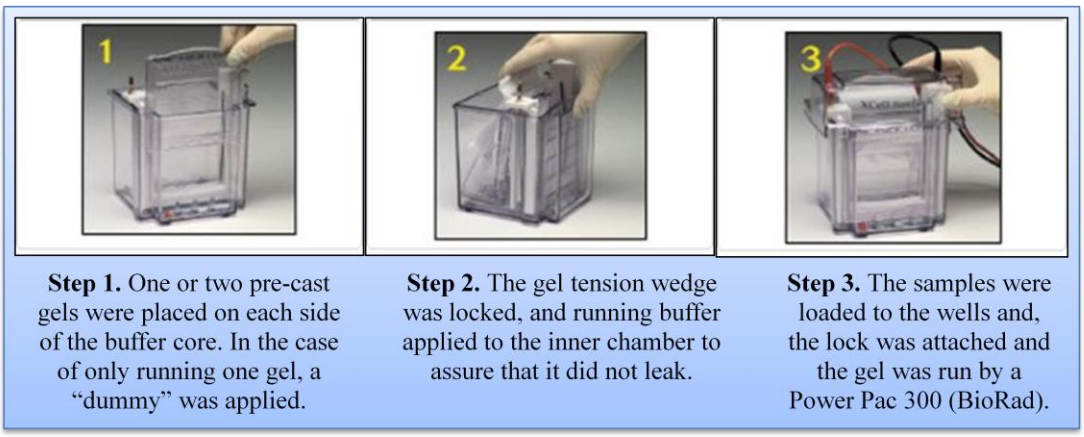

Figure 14. The setup of XCell Surelock™ Mini-Cell for separation of proteins by SDS-Page. Each step in the setup is described (adapted from (106)).

Step 2: Transferring the proteins to a Polyvinylidene difluoride (PVDF) membrane

In the second step the proteins were electro transferred to a PVDF membrane (Figure 13 D). Prior to use the pads and Watman™ chromatography papers (3mm, GE Healthcare, England) were soaked in blotting buffer (50 mL MeOH, 10 X blottingbuffer (30.3 g Tris (Bio-Rad, USA), 144 g Glycin (Merck, Germany), 1L dH_2O) + dH_2O to a final volume of 500 mL), and Immobilon® Transfer Membranes Polyvinylidene Difluoride (PVDF) (0.45µm pore size, Millipore, Germany) were activated in Methanol for 1 minute. The pads, watmans, gel and membrane were carefully placed into a transfer cell (XCell II™ Blot module, Life Technologies™, USA) as Figure 15 demonstrates, and placed in the transfer chamber (XCell SureLock™ Mini-Cell). The gel tension wedge was locked and the inner chamber filled with blotting buffer. The surrounding chamber was filled with ice water to prevent temperature fluctuation in the system during the blotting reaction as this may interfere with the transfer of the proteins. The apparatus was placed on ice at 4^0C and run at 400 mAmp for one hour on a Power Pac 300 (BioRad, USA). After 1 hour, the apparatus was dissembled, and the membrane was transferred to a chamber for blocking.

Order	1 Gel	2 Gels
1	2 Pads	2 Pads
2	Whatman	Whatman
3	Gel	Gel
4	Membrane	Membrane
5	Whatman	Whatman
6	Pad	Pad
7	3 Whatman	Whatman
8	2 Pads	Gel
9	-	Membrane
10	-	Whatman
11	-	2 Pads

Figure 15. The blotting chamber. The order of Pads, Whatman, Gels and membranes placed in the blotting chamber where the proteins on the gel are electro transferred to a polyvinylidene difluoride (PVDF) membrane (adapted from (106)).

Step 3: Blocking the membrane

To membranes were "blocked" to avoid unspecific binding of primary antibody to unoccupied spaces on the PVDF membrane, thereby preventing high background when developing the membrane. 10 mL of the appropriate blocking solution was added to the membrane and it was incubated at room temperature for 1 hour on a See-saw Rocker (SSL4, Stuart®, USA and UK). The blocking solution constituted of 5 % Bovine Serum Albumin (BSA) (SIGMA-ADLRICH, USA) or 5 % nonfat dried milk in Tris-Buffered Saline and Tween 20 (TBST) consisting of 0.15 M NaCl, 10mM UltraPure™ TRIS-HCl (Life Technologies™, USA) and 0.5 % Tween 20 (Merck, Germany) in distilled H_20. All blocking solutions are listed in Table 2.

TBST was not used when evaluating the B7-H3 protein levels, instead a buffer containing 0.5 % Tween in PBS to a total volume of 500 mL was used to prepare the blocking buffer and all subsequent solutions with primary and secondary antibody. Furthermore, this buffer was applied at all washing steps of the B7-H3 membrane.

Step 4: Incubation with primary and secondary antibody

To visualize the protein band immobilized on the membrane, the membranes were incubated with a primary antibody specific for the protein of interest, following incubation with an enzyme-coupled secondary antibody which detects the primary

antibody (Figure 13 E), F) and G)). The primary antibody was diluted in 5 % BSA in TBST or 5 % nonfat dried milk in TBST, and at dilutions recommended by the manufacturer. An overview of primary antibodies, dilution factor and solutions is presented in Table 2. The membranes were incubated overnight at 4°C under careful agitation on a Platform Rocker (Bibby Stuart STR6, USA and UK).

Table 2. The antibodies used in the Western blot analysis. All antibodies utilized in present thesis are listed here. All primary and secondary antibody dilutions were prepared in TBST, apart from the B7-H3 antibody where both primary and secondary antibody dilutions were prepared in 0.5 % Tween in PBS (for manufacturer see Appendix B).

Antibodies (Ab)	**Molecular weight (kDa)**	**dilution of primary Ab**	**Secondary Ab and dilution**	**Antibody dilutants and blocking buffer**
Akt	60	1:1000	Rabbit (1:2000)	5 % BSA
Phospho-Akt (Thr308)	60	1:1000	Rabbit (1:2000)	5 % BSA
Phospho-Akt (ser473)	60	1:1000	Mouse (1:5000)	5 % Milk
Phospho-Bad (ser112)	23	1:2000	Mouse (1:5000)	5 % BSA
Phospho-GSK-3β (ser9)	46	1:1000	Rabbit (1:2000)	5 % BSA
Phospho-mTOR (Ser2448)	289	1:1000	Rabbit (1:2000)	5 % BSA
Phospho-PDK1 (Ser241)	58-68	1:1000	Rabbit (1:2000)	5 % BSA
Phospho-elF4E	25	1:1000	Rabbit (1:2000)	5 % BSA
Phospho-p70S6K (Thr389)	70.85	1:1000	Mouse (1:5000)	5 % Milk
α-tubulin	55	1:5000	Mouse (1:5000)	5% Milk
β-actin	~ 42	1:1000	Goat (1:2000)	5% Milk
Human B7-H3	~100	1:1000	Goat (1:2000)	5% Milk

The subsequent day the membranes were washed three times in TBST for 15 minutes following incubation with the appropriate secondary horseradish peroxidase (HRP)-coupled antibody. The secondary antibody was diluted in 5 % non fat dried milk or 5% BSA in TBST for 1 hour at room temperature. The washing steps remove any remaining antibodies, and thus prevent unspecific binding. After incubation with the secondary antibody, the membranes were washed three times for 15 minutes in TBST. All washing steps were performed under gentle agitation on a See-saw Rocker (SSL4, Stuart®, USA) at room temperature.

β-actin and α-tubulin were used to control protein loading and transfer differences on all blots.

Step 5: Protein imaging using chemiluminescense

The secondary antibodies were coupled with a HRP-enzyme. The Supersignal® west dura Extended duration substrate (Thermo Scientific, USA) is a luminol-based enchanced chemiluminescense (ECL) HRP substrate which is used to detect HRP-enzyme activity, and provides a chemoluminescent signal that is stable for several hours and can be detected on a chemiluminescense imager (107). The two HRP substrate components were mixed at a one to one ratio to prepare the substrate working solution, and the blots were subsequently incubated with the solution for 5 minutes. Excess reagent was drained from the blots, and they were covered with a plastic sheet and imaged in a G-BOX chemi (Syngene, USA) using the Syngene Genesnap software (Figure 13 H). The exposure time varied from 20 seconds to 10 minutes to find the optimal image.

3. Results

3.1 Optimization of cell lines

Prior to the drug screening procedure the breast cancer cell lines MDA-MB-435 and MDA-MB-231 variants, shB7-H3 (silenced for the expression of the B7-H3 protein) and vector control cells TR33 (expressing the protein) were optimized for growth in 384 well plates for five days. The cells were lysed at day five by adding CTG, and luminescence was measured to quantify cell viability. The level of luminescence was plotted against increasing cell number (Figure 16). The optimal cell numbers are presented in Table 3.

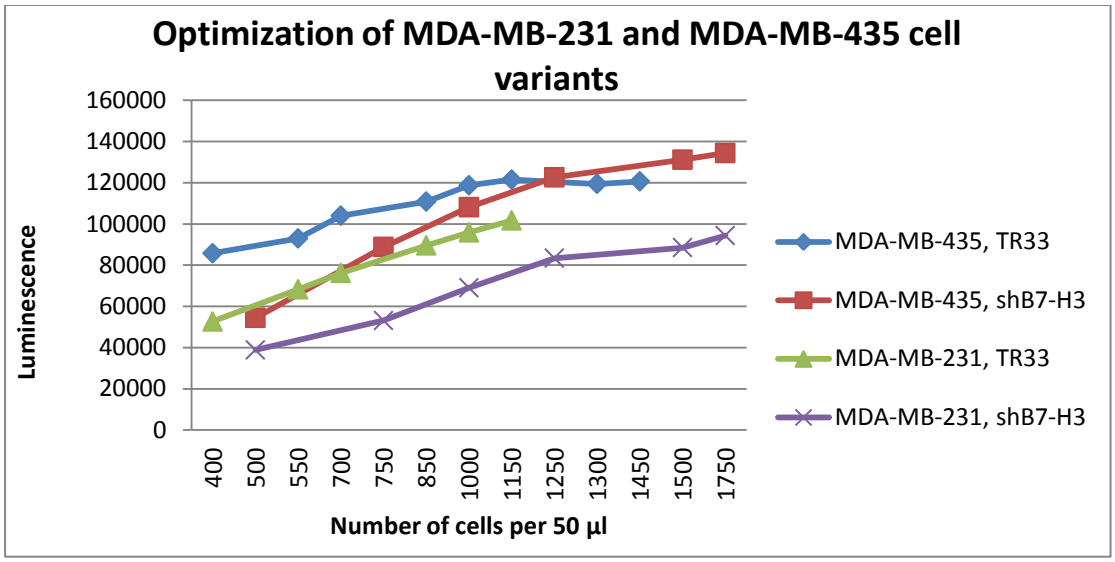

Figure 16. Growth curves of MDA-MB-435 and MDA-MB-231 cell variants. The X-axis presents the number of cells per well, whereas the Y-axis shows the measured luminescence levels. Each data point is an average of seven replicas. The TR33 vector control cells express the B7-H3 protein, whereas the protein is silenced in the shB7-H3 cells.

Table 3. The number of cells chosen for drug screening procedure in 384 well plates.

Cell line	Cell line variant	Cell number per well
MDA-MB-435	TR33	500
	shB7-H3	650
MDA-MB-231	TR33	750
	shB7-H3	900

3.2 Drug screening of breast cancer cells

The sensitivity of the MDA-MB-435 and MDA-MB-231 shB7-H3 cells were compared to the TR33 cells in order to study the putative effect of knockdown of the B7-H3 protein on drug response.

The cells were plated at their optimal numbers (Table 3) in 384 well plates containing 22 drugs at different concentrations printed in duplicate (Medical Biotechnology VTT, Finland) (Table 1). After 5 days of incubation cell viability was measured to evaluate the drug response. The drug screening was performed twice for each cell line variant, and the reproducibility of the duplicate screens was evaluated with respect to their correlation (Figure 17). A high correlation, ranging from 0.87 - 0.91, showed that the replicate screens were similar and thus biologically representative.

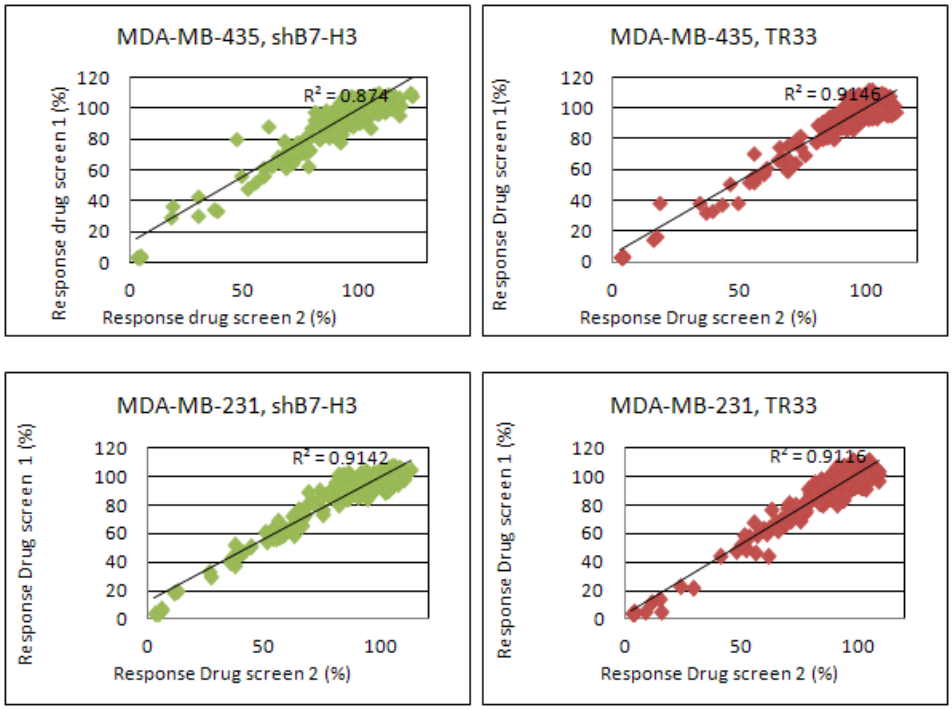

Figure 17. Scatter plots of two independent drug screening experiments for each cell line; MDA-MB-435 (shB7-H3 and TR33) and MDA-MB-231 (shB7-H3 and TR33). Satisfactory correlation between duplicate drug screens was observed. All data was normalized before the correlation was examined.

The cell lines were considered to be responsive to drugs that induced ≥ 20 % growth inhibition. This cutoff value was based on long-term experience with drug screening in 384 well plates from our collaborators in Finland. The percentage response of each

cell variant at the highest drug concentration is shown in Table 4 where a high response indicates high drug efficacy.

Several of the drugs had an effect on both MDA-MB-435 and MDA-MB-231; Bortezomib, Doxorubicin Hydrochloride and Radicol induced the highest response. These are inhibitors of the proteasome, topoisomerase 2 and Hsp90, respectively. Furthermore, several drugs targeting proteins in the PI3K/Akt pathway had a good response and induced over 20 % growth inhibition. In general, the drugs targeting different receptors were non-responsive in all cell line variants, with the exception of BIBW2992 and Lapatinib targeting the HER2 and EGFR (Table 4).

Table 4. The response (percentage) of each cell line variants upon exposure to the *highest* concentration of each drug. A drug response of 97 % indicates that only 3 % of cells were left in the well when compared to 100 % growth. The compounds, their targets, and the percentage response upon exposure to the highest drug concentration are shown. Blue colors indicate that the cells were non-responsive (per definition, < 20 % growth inhibition was used as a cutoff value as non-responsive), orange indicates 20 - 60 % response of the cell lines and yellow indicates drugs that induced > 80 % response in the cells.

Compound	Site of action	Response at the highest drug concentration (percentage)			
		MDA-MB-435		MDA-MB-231	
		TR33	shB7-H3	TR33	shB7-H3
Bortezomib	Proteasome	97	97	96	96
Doxorubicin Hydrochloride	Topoisomerase 2	96	95	96	94
Radicicol	Hsp90	84	73	87	85
BIBW2992	EGFR + HER2	67	68	51	58
API-2	Akt/PKB	31	45	50	63
Temsirolimus	mTOR1	47	48	47	49
Everolimus	mTOR1	39	36	41	42
PI 103 Hydrochloride	PI3K/mTOR	24	21	32	35
Wortmannin	PI3K	17	22	28	35
PD 184352	MEK/ERK	25	31	28	11
4-hydroxytamoxifen	ER	19	22	24	29
Lapatinib	EGFR + HER2	27	20	22	25
Akt 1/2 kinase inhibitor	Akt/PKB	5	8	23	21
Trastuzumab	HER2	21	18	20	22
UO126	MEK/ERK	4	0	25	18
CI-1033	Pan-ErbB	6	5	11	14
PD153035 Hydrochloride	EGFR	6	4	14	10
Symansis CP-724714	HER2	10	9	11	12
Bevacizumab	VEGFR	3	7	9	7
Gefitinib	EGFR	4	3	8	8
AAL-993	VEGFR	4	3	8	8
AG 538	IGFR	-2	1	3	6

The differences in drug response between the shB7-H3 cells and TR33cells at all drug concentrations in each cell line for the drugs that induced ≥ 20 % growth inhibition were investigated using a Student's t-test.

3.2.1 Drug response in MDA-MB-435 cell variants

The drug screening identified four different compounds that had significantly different efficacy in the MDA-MB-435 shB7-H3 cells compared to the TR33 cells. These drugs were API-2, an AKT inhibitor, Bortezomib, an inhibitor of the proteasome, Radicicol, an Hsp90 inhibitor and Doxorubicin hydrochloride, a Topoisomerase 2 inhibitor. Figure 18 presents the growth response curves of these drugs.

API-2 treatment showed a better efficacy in the shB7-H3 variants at the three highest concentrations; 200 nM ($p = 0.045371$), 2 µM ($p = 0.00166$) and 20 µM ($p = 0.00502$). A good effect of Bortezomib was seen in both cell variants, however at 52 nM ($p = 0.046136$) the efficacy was significantly better in the shB7-H3 cells. However, exposure to Radicicol resulted in a significantly better response in the TR33 cells at 2 µM ($p = 0.000467$) and 20 µM ($p = 0.032435$). Doxorubicin hydrochloride also had a better efficacy in the TR33 cells at 200 nM ($p = 0.003653$).

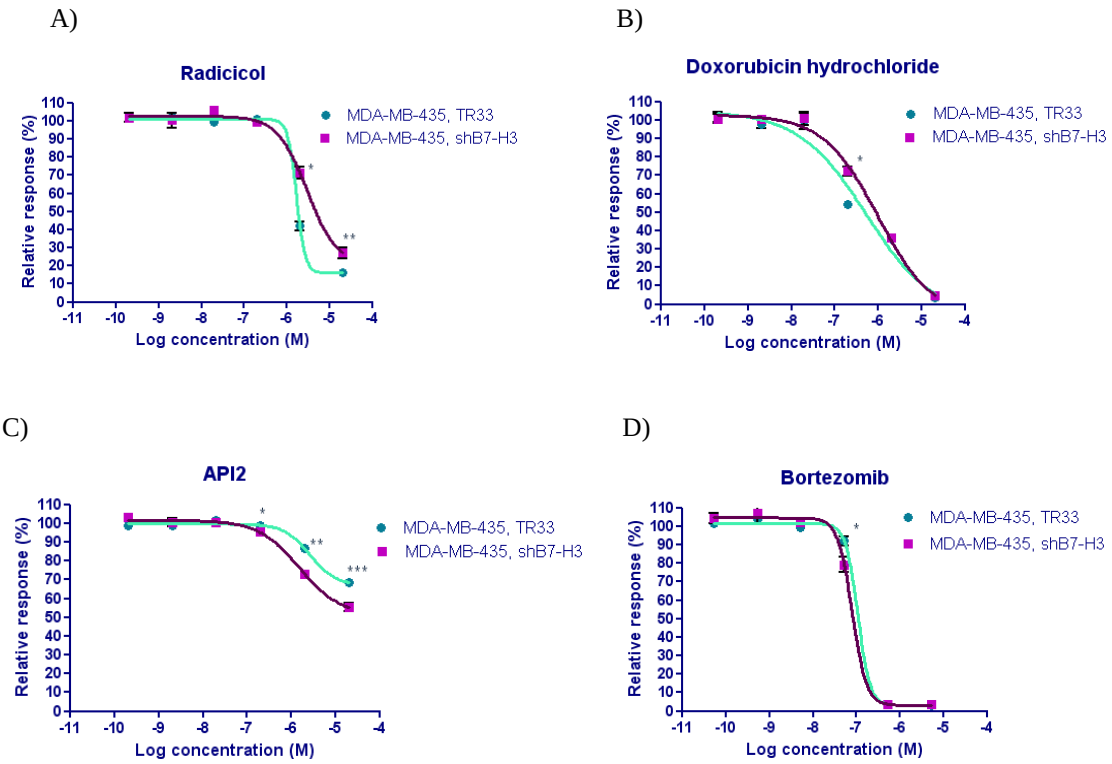

Figure 18. Growth response curves of the drugs with significant different efficacy in the MDA-MB-435 cell variants. The y-axis represents the relative response (%) versus the logarithmic concentration of the drugs on the x-axis. Green circles represent the response of the B7-H3 expressing cells and the purple squares show the response of the B7-H3 knockdown cells, shB7-H3. The figures show the growth inhibition upon treatment with A) Radicicol (*p = 0.000467, ** = 0.032435), B) Doxorubicin hydrochloride (*p = 0.003653), C) API-2 (*p = 0.045371, ** = 0.00166, *** = 0.00502) and D) Bortezomib (*p = 0.046136). All data has been normalized.

3.2.2 Drug response in MDA-MB-231 cell variants

Five different drugs were identified as having a significantly different efficacy in the MDA-MB-231 shB7-H3 cells compared to the TR33 cells. These drugs were API-2, Everolimus, an mTOR inhibitor, Doxorubicin hydrochloride and the MEK/ERK inhibitors UO126 and PD184253. The growth inhibition curves are shown in Figure 19.

Both API-2 and Everolimus showed a consistently better efficacy in the B7-H3 knockdown cells. API-2 had a better efficacy at 200 nM (p = 0.007852), 2 µM (p = 0.002208) and 20 µM (p = 0.000030) whereas Everolimus had a better efficacy at 20

nM (p = 0.019225), 200 nM (p = 0.001515) and 2 µM (p = 0.014489). Doxorubicin hydrochloride had a high effectiveness in both cell lines, but a better response in the B7-H3 knockdown cells at 200 nM (p = 0.000309) was observed. Although the small molecule inhibitors PD184352 and UO126 had minimal effect in any of the cell variants, the highest drug concentrations, 8µM (p = 0.001285) and 20 µM (p = 0.032548) respectively, showed a more pronounced effect in the TR33 cells.

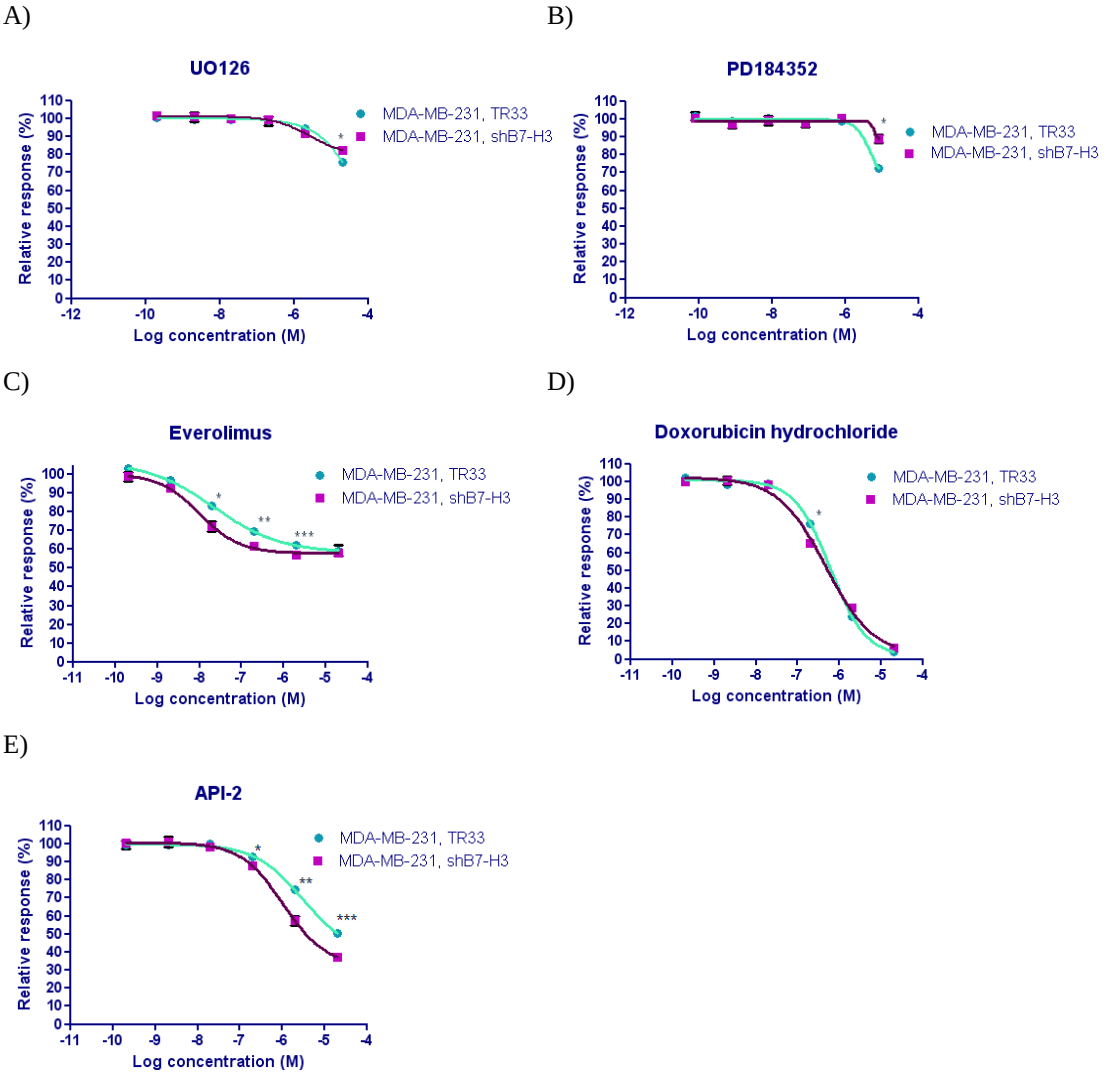

Figure 19. Growth response curves of drugs with significant different efficacy in the MDA-MB-231 cell variants. The y-axis represents the relative response (%) versus the logarithmic concentration of the drugs on the x-axis. Green circles represent the response of the B7-H3 expressing cells and the purple squares show the response of the B7-H3 knockdown cells. The graphs show the growth response upon treatment with the anti-cancer drugs A) UO126 (*p = 0.032548), B) PD184352 (*p = 0.001285), C) Everolimus (*p = 0.019225, ** = 0.001515, *** = 0.014489), D) Doxorubicin hydrochloride (*p = 0.000309) and E) API-2 (*p = 0.007852, ** = 0.002208, *** = 0.000030). All data has been normalized.

3.2.3 The half maximal effective concentration (EC_{50})

The EC_{50} is defined as the concentration of drug that shows a response halfway between the baseline and the maximum response of a dose-response curve (108). The EC_{50} values were determined from the dose-response curves, which usually follow a sigmoid shape (S-shape). If this shape were not achieved, for example due to lack of high enough drug concentrations to reach a maximum response, the calculation of an EC_{50} value would be ambiguous and therefore not calculated. The EC_{50} values of drugs with significant difference in the cell variants are presented in Table 5.

Table 5. The EC_{50} Values of MDA-MB-435 and MDA-MB-231 cell variants. N/A = Not analyzed because a maximum response was not reached. A square with a dash (-) indicate that there was no significantly different efficacy between the cell line variants, and EC_{50} values was thus not calculated.

Cell line	EC_{50} Values (µM)			
	MDA-MB-435		MDA-MB-231	
Variant	**TR33**	**shB7-H3**	**TR33**	**shB7-H3**
API-2	2.61	1.51	3.03	1.06
Doxorubicin Hyrdochloride	0.53	0.97	0.60	0.47
Radicicol	1.65	2.94	-	-
Bortezomib	0.11	0.08	-	-
Everolimus	-	-	0.02	0.01
UO126	-	-	N/A	N/A
PD184253	-	-	N/A	N/A

3.3 Confirmation of B7-H3 silencing in MDA-MB-435 and MDA-MB-231 cell variants

Western blot analysis showed the shB7-H3 cells had a very low expression of the B7-H3 protein compared to the TR33 cells in both cell lines tested, which demonstrated that the model system was adequate (Figure 20).

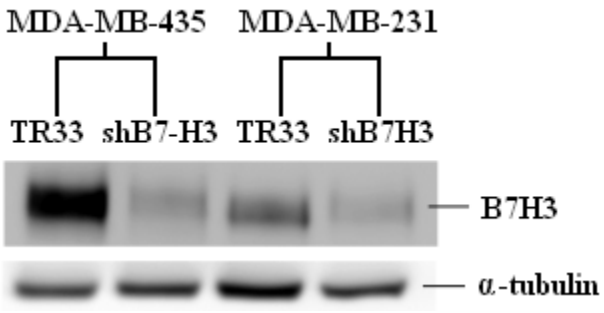

Figure 20. Western blot analysis confirming knockdown of the B7-H3 protein: Western blot analysis of the B7-H3 expression in MDA-MB-231 and MDA-MB-435 cell variants (shB7-H3 and TR33). The shB7-H3 cells showed a low expression of the protein compared to their TR33 counterparts. α-tubulin was used as loading control (The blot is representative of three independent experiments).

3.4 Western blot analysis of target proteins in the PI3K/AKT pathway

The drug screening revealed drugs that showed a consistently better response in the shB7-H3 cells. API-2 had a better effect in the shB7-H3 cells of both MDA-MB-231 and MDA-MB-435, whereas for Everolimus this was only shown for MDA-MB-231 shB7-H3 cells. These small molecule inhibitors were chosen for further investigation of the molecular mechanisms behind the difference in response.

The cells were exposed to these drugs for 0 hours, 0.5 hours and 2 hours before the phosphorylation levels of target proteins were examined. MDA-MB-435 cell variants were treated with 20 µM API-2, whereas the MDA-MB-231 cell variants were treated with either 2 µM API-2 or 200 nM Everolimus. These concentrations were achieved from the drug screening at concentrations with the most pronounced difference between the cell line variants. API-2 is a selective Akt inhibitor whereas Everolimus inhibits mTOR. Therefore we chose to examine the regulation of several proteins in the PI3K/Akt-mTOR pathway.

3.4.1 MDA-MB-435 cells treated with API-2 (20 µM)

The phosphorylation levels of elF-4E, Akt (ser473), mTOR and p70S6 kinase (p70S6K) were investigated in MDA-MB-435 cell variants treated with API-2 (20µM), but no differences were found between the cell variants (data not shown).

3.4.2 MDA-MB-231 cells treated with API-2 (2µM)

MDA-MB-231 shB7-H3 cells treated with API-2 showed a reduction in Akt phosphorylated at serine 473 (ser473). p-Akt is the active form of Akt where it can subsequently phosphorylate and regulate downstream targets (Figure 19). The phosphorylation of mTOR (activate mTOR) did not change at any time point after treatment with API-2 (Figure 21). However, a dramatic reduction in the phosphorylation level of a downstream target of mTOR, the p70S6K (active when phosphorylated), was seen in the B7-H3 knockdown cell variants (Figure 22).

In addition, the phosphorylation levels of several other central proteins in this pathway, elF4E, GSK-3β and BAD, were also studied, however no differences between the cell variants were observed (data not shown).

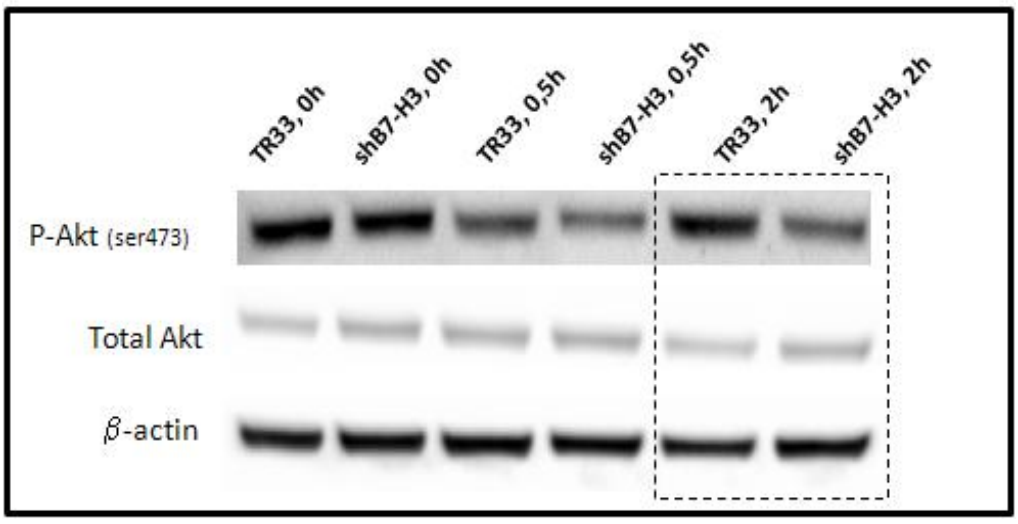

Figure 21. The effect of API-2 exposure (2µM) on phospho-Akt levels in MDA-MB-231 cell variants. The cell variants were exposed for 0 hours, 0.5 hours and 2 hours and protein activity was evaluated by comparing the cells at each time interval as indicated by the stippled box. The levels of phosphorylated Akt (p-Akt (Ser473)) decreased over time in the B7-H3 knockdown cells. Total Akt and β-actin were used as loading controls (The blot is representative of two independent experiments).

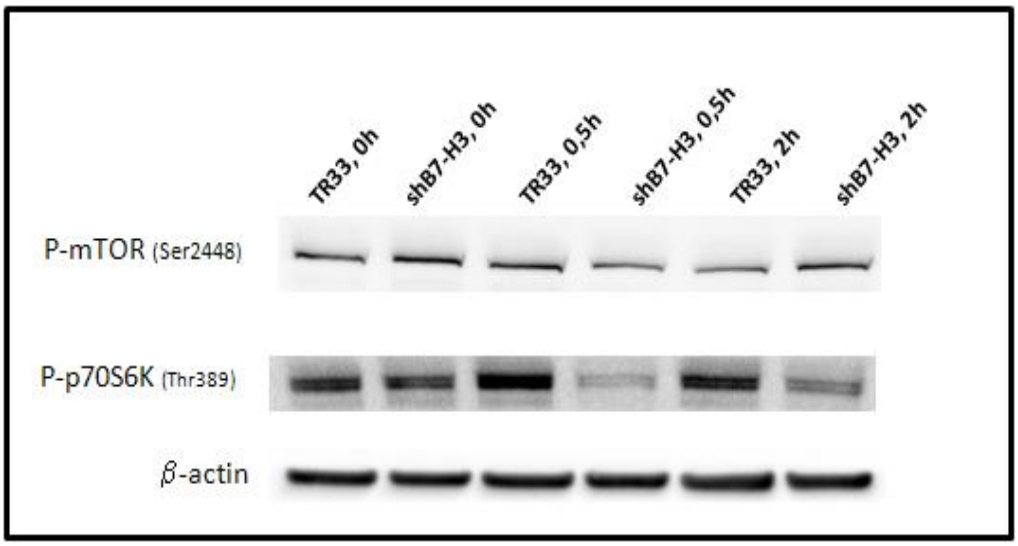

Figure 22. The effect of API-2 exposure (2µM) on phospho-mTOR and phospho-p70S6K levels in MDA-MB-231 cell variants. Cell variants were exposed for drugs for 0 hours, 0.5 hours and 2 hours. The blot showed no difference in p-mTOR levels, but a markedly decrease in phosphorylation level of the downstream target of mTOR, p70S6K. This was only observed in the B7-H3 knockdown variants, but not in the B7H3 expressing variants. β-actin were used as loading controls (The blot is representative of two independent experiments).

3.4.3 MDA-MB-231 cells treated with Everolimus (200 nM)

The MDA-MB-231 cells treated with Everolimus showed a reduction in p-p70S6K levels in B7-H3 silenced cells, but not in the p-mTOR levels of either cell variants (Figure 23). Interestingly, the levels of phosphorylated Akt (ser473) showed a dramatic increase in both cell variants upon treatment with Everolimus, however, this was less pronounced in the B7-H3 knockdown cells (Figure 24).

The levels of p-elF4E were also investigated, but showed no difference between the cell variants (data not shown).

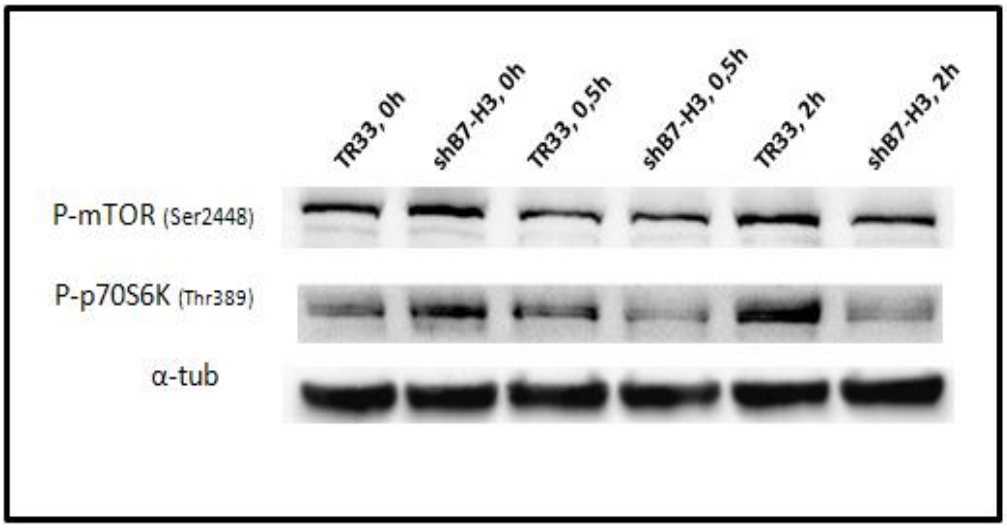

Figure 23. The levels of p-mTOR and p-p70S6K upon exposure to 200 nM Everolimus in MDA-MB-231 cell variants. The levels of p-mTOR did not change during exposure to the drug. A marked decrease in the phosphorylation levels of p70S6K was observed in the B7-H3 knockdown variants. α-tubulin was used as a loading control (The blot is representative of two independent experiments).

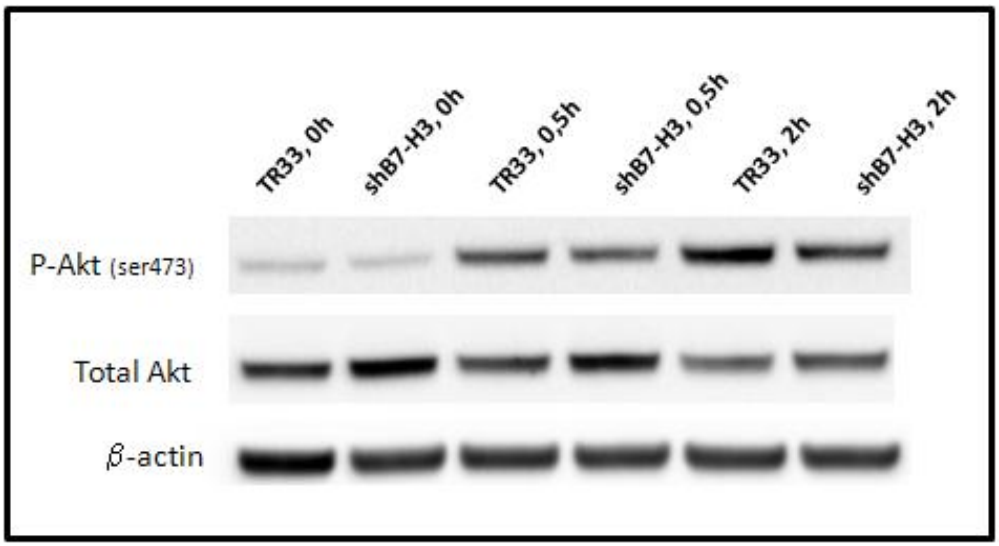

Figure 24. The levels of p-Akt upon exposure of 200 nM Everolimus in MDA-MB-231 cell variants. The levels of p-Akt (ser473) increased with time after drug exposure in both cell variants, and slightly less in the B7-H3 knockdown cells. Total Akt and β-actin were used as loading controls (The blot is representative of two independent experiments).

4. Discussion

4.1 Methodological considerations

4.1.1 *In Vitro* cell cultures

Cultured human cancer cell lines are valuable tools for functional studies in cancer as they have many of the same recurrent genomic and transcriptional characteristics as tumors (109). Therefore they are good models for experiments that are not possible to conduct in humans, both due to practical and ethical reasons. Cell lines are easily accessible, propagated and maintained, whereas primary tumors are of limited access. Furthermore, cell lines present homogenous cell populations, while primary tumors are heterogeneous with stroma consisting of infiltrating lymphocytes and other cell types, making the actual tumor cell percentage low. This may be a limitation of several models. However, cell lines can be manipulated by establishing specific phenotypes, like the B7-H3 knockdown model in the present thesis, making it possible to study both function and the impact of specific molecules on malignant processes. Moreover, in *vitro models* have also been shown to be predictive of *in vivo* drug response, emphasizing their relevance in cancer research (110).

The fact that cancer cell lines are genomically unstable makes it important to avoid long term culturing and high confluence levels, as this may influence the genetic composition, and thus effect the phenotypic properties, of the cells (111). When the cells become too confluent the lack of nutrition, space and the accumulation of waste might influence the gene expression. For example by for upregulating stress related genes and activating genes to resist apoptosis. By standardizing the culturing conditions using optimal culture medium, maintaining the cells at low passage numbers and at a confluence level of approximately 80 %, we tried to minimize the risk of genetic drift that might influence the results. In order to achieve reproducible and quantifiable results cells must also be propagated under well-defined experimental conditions (112). Moreover, established sterile techniques were used to prevent contaminations, and the cell lines were routinely checked for mycoplasma infections. Another aspect of *in vitro* cell cultures is the risk of cross-contaminations

(113). As the cells are used in experimental models as surrogates for their tissue of origin, their identity is important for the validation of data. The MDA-MB-435 and MDA-MB-231 cell lines were purchased from the American Type Culture Collection (ATCC), and have previously been authenticated in our laboratory (101).

It is important to take into consideration that cells are dynamic, living organisms that might for instance fluctuate in growth rate when conducting *in vitro* experiments. This makes it important to perform experiments several times and obtain reproducible results, which assures that any differences or effects observed are general, and not due to random events.

Although cancer cell lines are useful tools, they are only experimental models of human cancer, and thus have their limitations in entirely recapitulating the disease in humans. Breast cancer is thought to develop due to intrinsic properties of the tumor cells, as well as through interaction with cells and signaling molecules present in the microenvironment, and this crosstalk is also important in the process of metastasis (114). Clearly, the complex microenvironment is not recaptured in the *in vitro* setting. The work in the present thesis was performed in two dimensional (2D) cultures, which is a well-established procedure in our laboratory. Cells can also be cultured three dimensionally (3D) which presents an opportunity to assay cell behavior in a system that more closely resembles the *in vivo* setting (115;116). However, the work with 3D culturing is more laborious, and would require another experimental setup. The use of a 3D culturing system or xenografts could be used to stratify the results from the present experiments, as these experimental models provide a closer similarity to the disease in humans (112;115). In general, there are less ethical and practical considerations by the use of *in vitro* cell culturing opposed to *in vivo*, and although there use cannot fully replace xenografts, cell lines serve as valuable first line experimental models.

4.1.2 The origin of cell line MDA-MB-435

The origin of the cell line MDA-MB-435, used in our experiments, has been debated. It was initially derived from a patient with ductal adenocarcinoma, and was thus

identified as a breast cancer cell line (117). However, microarray derived data have indicated that the gene expression pattern of the cell line resembles that of human melanoma cells, which was confirmed in other studies (118;119). In contrast to these findings, there are also indications of the mammary epithelial origin of this cell line (120). The identification of co-expression of mammary epithelial cell and melanocyte markers has postulated that this is due to lineage infidelity (121). This has further been supported by additional studies suggesting that the MDA-MB-435 is indeed a breast cancer cell (122;123).

The aim of this study was to investigate the putative effect of the B7-H3 protein on anti-cancer drug resistance, which is a general feature of cancer cells. Despite the controversy regarding the origin of the MDA-MB-435 cell line, we chose to use this cell line as a model to study the role of B7-H3 in resistance. The cell line was already an established B7-H3 knockdown model utilized and verified in our laboratory (101;102). Moreover, another breast cancer cell line was included in our experiments and strengthens our findings and justifies the choice of models. Our result should, however, be up scaled and stratified in a larger sample size in order to investigate if the function of B7-H3 is a general phenomenon in anti-cancer drug resistance.

4.1.3 Drug screening of breast cancer cell lines

Cancer cells have a high degree of genomic diversity that contributes to their drug sensitivity. High throughput drug screening has been used to systematically identify genomic markers of drug sensitivity in cancer cells, and also as a tool to link genetic composition to drug response (124;125). Through drug screening, multiple cancerous processes can be investigated simultaneously, making the technique effective in the search for novel treatment strategies. In the present thesis we refer to a small scale drug screening where B7-H3 silenced and B7-H3 expressing cell lines were screened with 22 different compounds. This allowed the investigation of possible differences in drug efficacy between B7-H3 silenced and B7-H3 expressing cells, and thereby the investigation of the function of the B7-H3 protein in drug response.

The use of 384 well formats requires small amounts of drugs and other reagents, which makes it both cost-efficient and safer compared to experiments in larger scale, in example in 96 well plates. The small volumes of cells, drugs and other reagents that were utilized require accurate pipetting. A robot was used to print the drugs on the plates, and a reagent dispenser was used to add cells and CTG to the wells, making the procedure more demanding with regards to machinery. However, this accuracy in printing and dispensing of such small volumes is not possible to achieve manually, thus increasing the reliability of the results. The growth of cells in small volumes is more challenging due to the constriction it imposes on the microenvironment and nutrient medium, and evaporation may therefore influence cell growth. Although cells that grow *in vitro* lack a microenvironment compared to the *in vivo* setting, cells strongly rely on interaction with other cells in the culture through signaling molecules and cell-to-cell contact to grow and thrive. Thus, to achieve reliable results, the cells were carefully optimized to obtain the best cell seeding number for the 384 well formats for five day long experiments. This was chosen from the growth curves obtained in the optimization procedure, at the steepest point before the curve flattens. At this point the cells are in their logarithmic phase of growth, which means they are highly proliferative and they have enough space to divide. When the number of cells becomes too high and the wells are confluent, the limitation of nutrients and space will affect the cell viability, and cells will die off or cease growing. In addition, the confluence levels in the 384 well plates were observed in the microscope at the endpoint of each drug screen (confluence levels of approximately 70-80 % in the controls were regarded as satisfactory).

An edge-effect could be observed as a tendency of reduced cell growth at the outer wells of the plates (Figure 24). This phenomenon has previously been observed by our collaborators at Medical Biotechnology VTT in Finland, and was taken into consideration in the design of the plate. Thus, there were no drugs in the outer wells. However, the plate-specific growth pattern made the outer wells inappropriate as controls. The lowest concentration of drugs (two middle rows, Figure 25) was therefore used as a reference of 100 % growth. Although the use of drug-free controls in theory would be beneficial, no growth inhibition was observed at the lowest concentrations, and therefore they were considered adequate controls.

The drugs were printed in different dilutions which made it possible to make growth inhibition curves and calculate EC_{50} values directly from the curves. Different levels of luminescence could be observed for each cell line, however all data was normalized against 100 % growth before the cell lines were compared thus correcting for differences in luminescence levels between the different screenings.

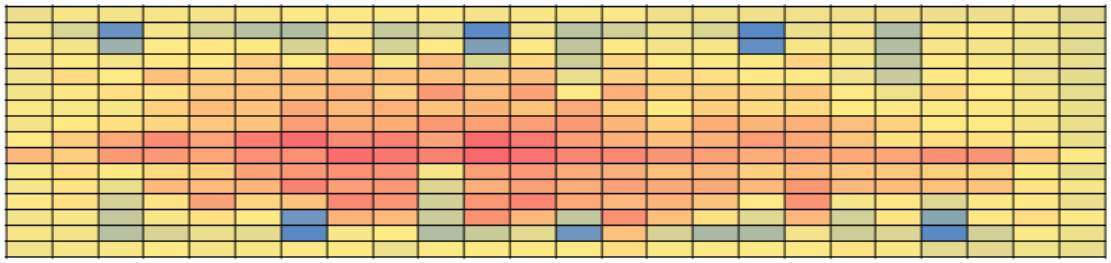

Figure 25. A heatmap of a drug screening plate. The colors represent levels of luminescence which reflects drug effect. Low levels (Blue) indicate low growth, yellow represents intermediate levels and orange/red represents high levels of luminescence and high cell viability. A tendency towards better growth in the middle, and less growth towards the edges was observed.

In our experiment, cell viability was used as an endpoint to measure the drug response. There are several other methods of measuring drug efficacy, for example by measuring the levels of apoptotic proteins. However, many of the drugs that were utilized are small molecule inhibitors which in many cases reduce cell growth (cytostatic) and do not directly induce apoptosis (cytotoxic), and cell viability was therefore considered to be a more suitable endpoint in this assay.

4.1.4 Western blot analysis of proteins

Protein activation levels were assayed by Western blot analysis. There are many antibodies available targeting numerous proteins, and at specific phosphorylation sites, allowing the investigation of both total protein levels in cells, and the degree of phosphorylation and thus the activity. However, the investigation of phosphorylated proteins can be cumbersome. As protein activity by phosphorylation is a dynamic process, precautions must be taken to prevent the dephosphorylation of proteins in the samples, and the harvesting of cells is an essential element in this process. Proteins may be altered with respect to phosphorylation when harvested enzymatically, thus other harvest methods are recommended when blotting of phospho-proteins (126). A

broad spectrum of phosphatase and protease inhibitors were added to the buffer when obtaining and lysing the cell pellets. In addition, the cells were kept on ice and detached by using a cellscrape to minimize dephosphorylation and degradation of proteins.

Optimizing the procedure with regards to cell lysing, as described above, sample amount, buffer conditions, dilutions of primary and secondary antibodies, and blocking reagent, may be necessary to obtain successful results. To achieve good results established Western blot analysis methods were utilized, either as provided by the manufacturer or established in our laboratory.

Cross reactivity of primary and secondary antibody is another challenge in Western blotting, which means that an antibody may recognize and bind other proteins than it initially is targeted for on the membrane. This can occur if the proteins share the same epitope recognized by the antibody, and may produce high background, unclear bands or multiple bands. The blocking solution and the concentration of antibodies used are often of importance with regard to this, and all blocking solutions and antibody dilutions was prepared as recommended by the manufacturer.

As described above, there are multiple challenges when performing Western blot analysis, which we also encountered in the detection of phosphorylated Akt at Threonine 308. As both phosphorylation of Akt at Thr308 and Ser473 is required for its full activation, we wanted to investigate both residues, since this would best reflect the activity of Akt. However, we were not able to detect any bands with our antibody. This might be due a number of technical issues, for example old antibody or the need of careful optimization. However, the investigation of downstream molecules of Akt is also a good way to assay protein activity. Thus, the detection of regulation of proteins downstream of Akt was regarded as indicative of reduced kinase activity. Futhermore, the phosphorylation of Akt at Ser473 has been used to detect activated Akt in a wide panel of studies, and also as a demonstration of prognostic significance of Akt activation (127). This, together with an observed corresponding decrease in phospho-Akt (Ser473), further strengthens the indication of an observed reduction in activity of the protein.

The cells were treated with different concentrations of the drugs API-2 and Everolimus before Western blot analysis was performed in order to identify any differences in protein regulations. The different drug concentrations were selected based on the growth inhibition curves at concentrations that showed the largest difference between the shB7-H3 and TR33 cells. At these points, it was postulated that the differences in regulation levels would be more pronounced.

In the initial experimental design the cells were incubated with drugs for the same time as the duration (five days) of the drug screening before protein activation levels were analyzed. However, no consistent results were found. API-2 and Everolimus have in previous studies been shown to induce an effect *in vitro* after 0.5 hours (128;129). Therefore, a new experimental design was chosen in order to better evaluate the immediate difference in response between the B7-H3 knockdown and B7-H3 expressing cells. We were interested in investigating the differences in response with regards to activity levels of proteins in the PI3K/Akt pathway, and not the total protein levels. The regulations of signaling molecules are rapid and dynamic and thus to better investigate the response with regards to protein phosphorylation levels upon drug exposure, we chose to treat cells for 0 hours (as a reference to no treatments), 0.5 hours and 2 hours. In general, all blots should be performed three times to ensure that the results observed are biologically reproducible, and not biased by other factors, such as timing, cell cycle or experimental design. All Western blot results represented in this thesis have been performed twice on biological replicates (cells seeded and treated in separate experiment), and hence they must thus be considered as preliminary results. However, the consistency in the Western blot analysis is promising, and further analysis will be performed to validate the results.

4.2 Biological considerations

In the present study it was shown that knockdown of the B7-H3 protein increased the sensitivity of two triple negative metastatic breast cancer cell lines, MDA-MB-231 and MDA-MB-435 to API-2, a selective Akt inhibitor. MDA-MB-231 B7-H3 silenced cells were also sensitized to Everolimus, an mTOR inhibitor. This was shown to be, at least partially, due to B7-H3 associated regulation of targets in the PI3K/Akt pathway in the MDA-MB-231 cells. More specifically the phosphorylation

of molecules, such as p70S6K and AKT, was decreased by B7-H3 silencing thus abrogating downstream protein translation and cell growth.

B7-H3 is an immunoregulatory protein which has previously been shown to have both inhibitory and stimulatory functions with regards to T-cell activity. Its expression has been associated with poor prognosis and advanced disease in a number of different tumor types, including in breast cancer (89;97;98). Regardless of its regulatory immunological functions, novel non-immunological roles of this protein in tumor biology have been identified. Chen *et al* demonstrated that B7-H3 expression correlated with increased migration and invasion *in vitro* (100), and this has also been confirmed by *in vivo* studies where a decreased metastatic potential was seen in nude mice injected with B7-H3 silenced cancer cells (101). A connection between the expression of B7-H3 and the resistance to the chemotherapeutic drug Paclitaxel in breast cancer has recently been demonstrated, where B7-H3 protein knockdown sensitized the cells to this compound both *in vitro* and *in vivo* (102). This, together with evidence from the present thesis, where silencing of the B7-H3 protein increased the sensitivity of breast cancer cells to two small molecule inhibitors, may indicate a more general association between B7-H3 expression and resistance. Hence the B7-H3 protein may be a putative prognostic and possible therapeutic marker.

The growing understanding of cancer cell biology has identified several pathways and molecules which are frequently highly expressed in cancer. These pathways are necessary for the growth and/or survival of certain cancers, which has fuelled the development of targeted therapy specifically inhibiting components of signaling pathways (130). Targeted therapy is different from conventional therapy in its specificity towards particular features of the tumor cells. Tamoxifen, Trastuzumab and Lapatinib are examples of such therapy that are currently used in the clinical setting against tumors overexpressing the estrogen and the HER2 receptor, respectively. Targeted therapy consists of antibodies, like Trastuzumab, but also a group of compounds called small molecule inhibitors, which inhibits components in intracellular signaling pathways frequently activated in human malignancies. This therapeutic approach presents a step towards a more personalized treatment strategy where the therapy could be tailored based on the genes and proteins that are deregulated in an individual patient's tumor. This approach has thus the potential to

increase the efficacy of cancer treatment and reduce the adverse side effects of conventional therapy (130).

Several of the compounds used in this study are categorized as targeted therapy. They included anti-cancer drugs targeting the ErbB receptor family like the EGRF, HER2 and HER4 receptor, but also drugs targeting the IGFR2, ER and VEGFR receptors. These receptors are widely implicated in many human malignancies, including breast cancer. For example, the ErbB family is frequently upregulated in breast cancer, and is one of the main signaling pathways where targeted therapy is being developed (130;131). Moreover, small molecules inhibiting PI3K, Akt, mTOR and MEK/ERK, which act downstream of these receptors (except the ER receptor) were included in the drug panel, in addition to three anti-cancer drugs targeting the proteasome, HSP90 and topoisomerase II, respectively. The PI3K/Akt pathway has been implicated in chemoresistance in breast cancer cells, and compounds targeting this signaling pathway were therefore of interest when investigating the putative impact of B7-H3 on anti-cancer drug resistance (86). Several of these are new substances and their clinical significance remains to be established, whereas some are already approved in the treatment of breast cancer, such as Lapatinib and Trastuzumab, or other types of cancers, such as Temsirolimus, Everolimus**.**

In general, targeted therapy have shown limited effect as single agents, and are often used in combinations with other targeted agents or conventional therapy, where they have shown to increase the treatment efficacy. For example, the combination of Paclitaxel with the dual HER2/EGFR tyrosine kinase inhibitor Trastuzumab and the HER2 inhibitor Lapatinib significantly improved the complete pathological response in women with HER2+ breast cancer as compared to any of the treatments in combination with Paclitaxel alone (132). In line with this combinatorial approach we wanted to investigate if the knockdown of the B7-H3 protein could be involved in regulating the response to any of the anti-cancer compounds used in the screen, and showed that knockdown of B7-H3 in combination with API-2 or Everolimus seemed to be more effective than administering the small molecules alone when cells overexpress B7-H3. The observed sensitization upon combinatorial inhibition emphasizes the complexity of cancer treatment and the potential of a combinatorial approach to improve patient outcome (127).

Several of the substances in the drug screening showed an effect on the cell lines as defined by the > 20 % cutoff level. The best responses were seen upon treatment with Bortezomib, Doxorubicin Hydrochloride and Radicol. The cell lines used in the present thesis are triple negative breast cancer, and are thus not expressing the ER, PR or HER2 receptors. However, the dual EGFR + HER2 inhibitor BIBW2992 had relatively good response in both cell lines, but in general the drugs targeting receptors showed a low response, and the majorities were considered non-responsive. As the aim of the drug screen was to investigate the effect of B7-H3 knockdown on drug response, the anti-cancer drugs that showed a continuously better effect in the B7-H3 knockdown, as compared to the B7-H3 expressing cells, were chosen for further investigation of the underlying molecular mechanisms. The downregulation of B7-H3 expression increased the effect of API-2 and Everolimus, which specifically inhibits targets in the PI3K/AKT pathway, AKT and mTOR respectively. In line with this we have previously observed that B7-H3 silenced breast cancer cells were more sensitive to the drug Paclitaxel by, at least partially, abrogating the Jak2/Stat3 signaling pathway (102). Thus our findings further confirm the ability of B7-H3 to modulate intracellular signaling.

The PI3K/Akt pathway is constitutively active in many human cancers, including breast cancer (76). This has stimulated the development of many small molecule inhibitors targeting components in this pathway (127). Akt/Protein Kinase B Signaling Inhibitor-2 (API-2/Triciribine) is a highly selective Akt kinase inhibitor which inhibits the phosphorylation, activation and signaling of the three Akt isoforms; Akt1, Akt2 and Akt3. It was identified as a specific Akt inhibitor suppressing cell growth and inducing apoptosis preferentially in human cancers with constitutively active Akt signaling (128). So far, API-2 has been combined with standard chemotherapies or radiation in preclinical studies (127) . Everolimus (RAD001) is a rapamycin analogue that inhibits mTOR1 activity (rapaloge) (129). This is mediated through Everolimus binding to the FK506-binding protein-12 immunophilin (FKBP-12), and this complex subsequently binds to a specific site near the catalytic site of mTOR and inhibits the phosphorylation of its downstream substrates through a poorly described mechanism (133). The drug is marketed as Affinitor (Novartis) and is

approved for the treatment of advanced kidney cancer and recently also other cancers (Approved by the U.S Food and Drug Administration (FDA) (134)).

To investigate whether we could relate the observed sensitization upon B7-H3 knockdown to activity levels of proteins in the PI3K/Akt pathway we performed Western blot analysis. An overview of the target proteins and the pathway are illustrated in Figure 26. The MDA-MB-231 B7-H3 knockdown cells showed decreased levels of phosphorylated Akt (Ser473) compared to the B7-H3 expressing cells upon treatment with API-2. mTOR1 is a central sensor of nutritional status and determines whether the cell should grow, and Akt signaling through mTOR1 plays an important role in the regulation of cell growth, proliferation and survival (130). Analysis of the phosphorylation levels of mTOR did not show any difference upon API-2 treatment. However, the downstream target of mTOR, the protein 70 S6 kinase (p70S6K), showed a dramatic reduction in activation level in B7-H3 silenced cells. p70S6K is a major stimulator of cell growth by promoting translation of ribosomal proteins and other transcriptional elements, and is activated by mTOR mediated phosphorylation (129). The observed decrease in phosphorylated p70S6K in the B7-H3 knockdown cells thus might, in part, explain the increased sensitization in the shB7-H3 cells upon API-2 treatment. A reduction of the phosphorylation levels of p70S6K was also seen in the MDA-MB-231 B7-H3 knockdown cells treated with Everolimus, whereas no differences were observed in the phosphorylation levels of mTOR. P70S6K has also been indicated as a biomarker of mTOR inhibition (135), as rapaloges has been demonstrade to predominantly inhibit mTOR signaling trough p70S6K phosphorylation (129). This implies that there might be a B7-H3 induced regulation of proteins in this pathway, and that knocking down B7-H3 increased the sensitivity to either drug via the same mechanism.

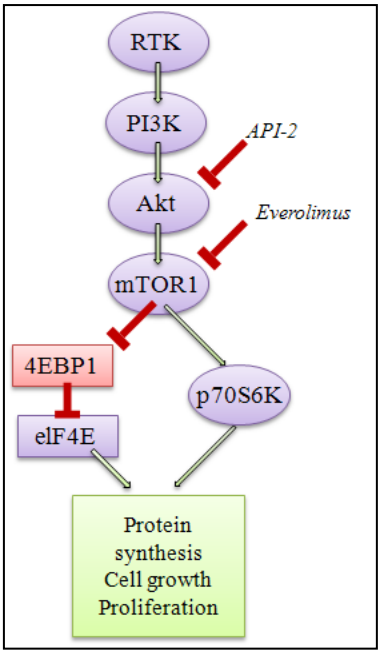

Figure 26. A simplistic overview of the PI3K-Akt-mTOR1 signaling pathway. The activation of this pathway leads to protein synthesis, cell growth and proliferation. The inhibitory effect of API-2 and Everolimus are indicated.

Several studies have shown that mTOR inhibition has resulted in a compensatory upregulation of Akt, thus limiting the effect of drugs targeting mTOR. O'Reilly *et al* demonstrated that Everolimus treatment induced the expression of Insulin receptor substrate-1 (IRS-1) (a positive regulator of the PI3K/Akt pathway) and increased Akt activation in both cancer cell lines and patient tumors (136). In line with this, we observed an upregulation of p-Akt levels (Ser473) in both vector control and B7-H3 silenced cells upon mTOR1 inhibition with Everolimus. This effect might be explained by the abrogation of a p70S6K dependent negative feedback loop that inhibits PI3K/Akt signaling. Hyperphosphorylated p70S6K inhibits IRS-1, an upstream activator of PI3K/Akt signaling, thus reducing Akt activity (137). An inhibition of mTOR results in decreased phosphorylation of p70S6K, thus abrogating the negative feedback loop, resulting in increased Akt activity. This contradictory effect of mTOR inhibition on Akt activity, in addition to its predominant cytostatic effect, may explain the limited effect of mTOR1 inhibitors as single agents in cancer management. However, dual inhibition of mTOR1 and Akt could, in theory, reverse this effect.

Compensatory upregulation of oncogenic pathways is well known, and has been shown in several studies. For instance, it has been demonstrated that Akt inhibition induced signaling through the MAPK/ERK pathway (138). Limitations of targeted therapy as single agents can therefore be explained by the fact that cancer cells can have oncogenic pathway redundancy, where multiple pathways are able to sustain tumor growth and development. Moreover, many small molecule inhibitors, such as Temsirolimus and Everolimus, are primary cytostatic substances, meaning that they will suppress cell growth, but not necessarily induce apoptosis. The plasticity and the extensive crosstalk within cellular pathways emphasize that multiple, rather than single agent targeted therapy, probably is a more efficient approach (Figure 27). By inhibiting multiple signaling pathways simultaneously resistance induced by intracellular crosstalk and redundancy can be circumvented. Hence, the understanding of the underlying molecular mechanisms of drug response is crucial to rationally combine treatment to the individual tumor.

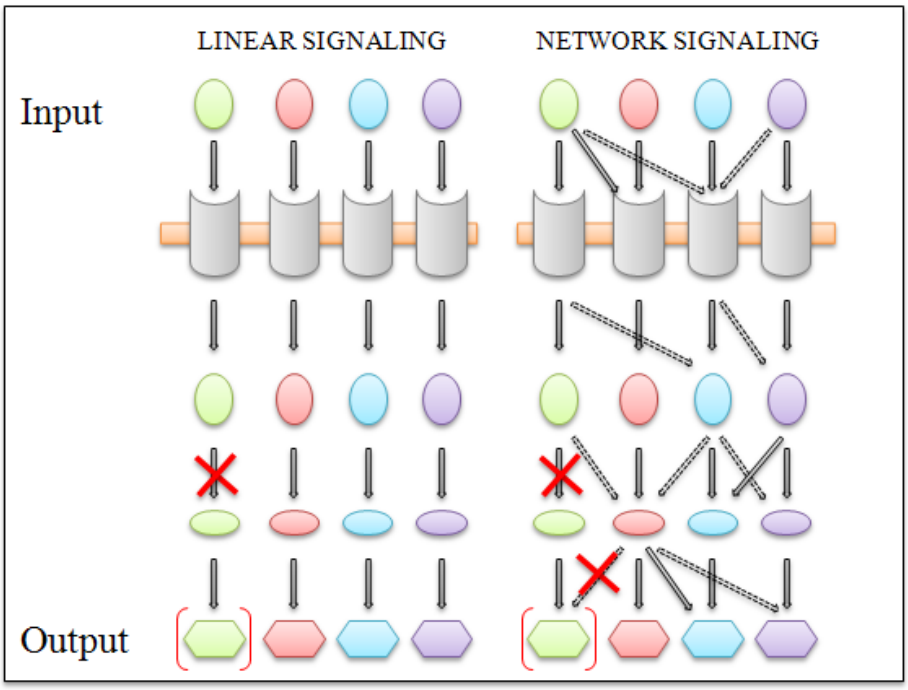

Figure 27. Cellular signaling. Cell signaling is complex, and is not linear but consists of a complex network with crosstalk and regulation. The abrogation of one malignant pathway might therefore be insufficient to abrogate a malignant signaling pathway, here illustrated in green, emphasizing the combinatorial approach of drug design. Importantly, to be able to rational design treatment, the complexity of signaling cascades needs to be investigated further (Modified from (139)).

Together, our results imply that the sensitization observed in the B7-H3 silenced cells upon treatment with API-2 and Everolimus is, at least in part, mediated through abrogating the Akt-mTOR1-p70S6k pathway in the MDA-MB-231 cells, resulting in decreased cell growth and proliferation through inhibiting protein translation. However, the specific role of B7-H3 in this context needs to be investigated further.

The genetic composition of the cell lines may also contribute to the drug response. The MDA-MB-435 cell lines showed no significant difference in response between B7-H3 knockdown and B7-H3 silenced cells upon treatment with Everolimus. Although both cell lines used are triple negative and initially have a high expression of the B7-H3 protein, they have characteristic genetic compositions with different gene expression patterns contributing to their response. This is further exemplified by the fact that although both cell lines showed an increased sensitization to API-2 treatment in the B7-H3 knockdown cells, no correlation with respect to activity levels of proteins in the pathway upon API-2 exposure has so far been found in the MDA-MB-435 cells. Clearly, the identification of mechanisms behind the increased sensitization to API-2 treatment shown in the MDA-MB-435 B7-H3 silenced cells can add further aspects to our findings. Moreover, the knockdown cells showed decreased proliferative rate in both cell lines, as observed by their different cell seeding number. This was also evident in the culturing of the cells where all knockdown cells had a slower growth than their B7-H3 expressing counterparts. This further emphasizes the importance of elucidating the function of B7-H3 in cell signaling.

Several of the anti-cancer drugs in our screen targeted the same proteins in the cells, however they induced different cellular response. For example, in addition to API-2 and Everolimus, there were two other compounds targeting Akt and mTOR, namely Akt 1/2 kinase inhibitor and Temsirolimus respectively. The MDA-MB-435 cell variants were non responsive to the Akt 1/2 kinase inhibitor (as demonstrated by a growth inhibition effect below 20 %), whereas the MDA-MB-231 cell variants had a minor response with 23 % (TR33) and 21 % growth inhibition at the highest concentrations. This was in contrast to the response to API-2 which induced a growth inhibition ranging from 31- 45 % in the MDA-MB-435 cells and 50-63 % in the MDA-MB-231 cells at the highest concentration (Table 4). The mechanism of action

of both Akt inhibitors is poorly understood, but it has been implicated that both substances bind to the PH-domain of Akt, thus preventing its translocation and activation at the plasma membrane (76). The Akt 1/2 kinase inhibitor has isozyme selectivity, and more effectively inhibit Akt 1 and Akt 2, respectively. Moreover, this inhibitor has also shown to have no effect in Akt that lack the PH-domanin (140). Because both inhibitors work in a PH-dependent manner, it is possible that these cell lines have a high expression of Akt 3, which is more effectively inhibited by API-2. Similarily, both Temsirolimus and Everolimus are Rapamycin analogues, and putatively inhibits mTOR1 through the same mechanisms. In theory analogue drugs are expected to exert the same effect, however there are many mechanisms that might explain variations between drug responses. The drugs may bind to their target protein with different affinity or have different stability in the cells. Furthermore, cells may harbor a specific mutation in the target protein which renders it resistant to the drug by interfering with drug binding, and thus make it less/not effective. The drugs may also have several mechanisms of action in the cell, inhibiting similar protein structures, and thus show differences in effectiveness. Therefore both the genotype of the cells and properties of the drug may influence the response to the drugs (38). The genetic composition of the cell may also interfere with drug efficacy. For example, Everolimus is a good substrate for the multidrug-resistance pump P-glycoprotein, and an intrinsic high expression of this protein might render the cells less responsive to this anti-cancer drug (129).

In this thesis, we have investigated the drug response in two triple negative breast cancer cell lines with respect to their expression of the B7-H3 protein. Triple negative breast cancer has an aggressive clinical course, and because they do not express any known molecular markers that are developed treatment against, their systemic management is limited to conventional chemotherapy. They represent a heterogeneous group of cancers, as our results demonstrate, where two triple negative cancer cell lines showed different responses upon treatment with different drugs. This is probably due to diverse genomic backgrounds in the cell lines, which contributes to their response. The classification of biomarkers that can identify the patients that will benefit from a treatment, or not, is therefore crucial. Moreover, the identification of novel effective therapeutic markers that can better target these aggressive tumors is important to improve the outcome for these patients. The future of breast cancer

treatment aims to develop individual treatment strategies based on the patient's genomic and phenotypic background, and thus to personalize the therapy. As demonstrated by the different response in two triple negative breast cancer cell lines in the present thesis, this could have a major impact on improving diagnosis and finding the ideal treatment regimen. However, the screening of individual patients to achieve their genomic profile presents a big challenge with respect to cost and work, and is not performed routinely today. Furthermore, more knowledge about the molecular mechanisms in breast cancer is needed before this can become reality. Targeted therapy is indeed a step towards a more personalized treatment strategy, but, as the present thesis illustrates, it is important to identify biomarkers, both genes and molecules, which can help predict outcome, response to treatment or serve as a therapeutic target.

5. Conclusion

Resistance to treatment is a general problem in advanced breast cancer, and increased knowledge about the underlying molecules and pathways involved in resistance is needed to improve the outcome for these patients. The identification of biomarkers of prognostics and predictive value is crucial in order to improve current cancer management.

In this thesis we showed that the silencing of the B7-H3 protein sensitized triple negative metastatic cancer cells to two small molecule inhibitors targeting the PI3K/Akt/mTOR pathway, a pathway that is frequently activated in breast cancer. Further investigation showed that the increased sensitivity was associated with B7-H3 induced regulation of molecules in this pathway. In the MDA-MB-231 knockdown cells a decrease in phosphorylated Akt was seen upon API-2 treatment as compared to their B7-H3 expressing counterparts. This was also reflected downstream of Akt with lower activity levels of the protein translation activator p70S6K. In the Everolimus treated MDA-MB-231 cells there was also a reduction in the phosohorylation levels of p70S6K. This might indicate a similar B7-H3 mediated mechanism of sensitization to both API-2 and Everolimus. The inhibition of mTOR induced a compensatory upregulation of phosphorylated Akt (ser473) in both the B7-H3 expressing and the B7-H3 knockdown cells. This effect might explain the lower effect of Everolimus treatment in the cell line, as compared to API-2. This exemplified that a combinatorial approach might be necessary to abrogate malignant pathways and circumvent resistance induced by intracellular crosstalk and pathway redundancy. In addition, the understanding of the underlying molecular mechanisms of drug response is crucial to rationally combine treatment to the individual tumors.

The previously observed relationships between B7-H3 expression and advanced disease and poor prognosis indicate that this protein can serve as a prognostic and predictive biomarker. Our results, together with the identification of the involvement of the B7-H3 protein in metastasis and chemoresistance, further imply that it might also be a suitable therapeutic target to increase the effect of anti-cancer drugs.

6. Future perspectives

The work in the present thesis demonstrated that knockdown of the B7-H3 protein increased the sensitivity of triple negative breast cancer cell lines to two small molecule inhibitors. To confirm these findings and to verify that our results reflect an important functional property of the B7-H3 protein, this needs to be investigated further in a larger panel of cancer cell lines. Furthermore, the experiments should also be validated in 3D culturing systems and ultimately in xenograft models, where the microenvironmental influence can be taken into consideration.

In previous studies, the silencing of the B7-H3 protein mediated an abrogation of the Jak2/Stat3 pathway. In this thesis we identified a role of the B7-H3 protein in the PI3K/Akt signaling pathway. The finding of several molecules that are apparently directly or indirectly regulated by B7-H3 may in turn help elucidate the exact biological function of this protein. It would therefore be of interest to investigate whether any molecules in the Jak2/Stat3 pathway might be affected upon API-2 and Everolimus treatment, as this could help unravel possible signaling crosstalk between these two pathways and the link to the B7-H3 protein.

In this thesis the activity levels of several proteins in the PI3K/Akt/mTOR pathway were investigated, and we intend to further confirm these findings on order to make the results suitable for publication. Also, the investigation of the cellular mechanisms underlying the increased sensitization of API-2 in the MDA-MB-435 cells is ongoing and the results may add further aspects to the biological role of the B7-H3 protein.

We have here investigated the treatment response of the cells at the protein level. It would be of interest to study the mRNA and miRNA genome wide expression profiles in the B7-H3 cell line models to learn more about the pathway implicated by B7-H3. In addition, we can further evaluate this by exposing the cell variants to API-2 and Everolimus. As we have illustrated in our work, cellular signaling is complex, and investigating alterations in gene expression levels might help create a more complete picture of the B7-H3 protein in cell signaling, and any findings can then be confirmed at the protein level by Western blot analysis. The integration of this knowledge with

current information can also help elucidate important mechanisms of resistance to therapy and metastasis.

References

(1) Alberts B, Johnson A, Lewis J, Raff M, Roberts K, Walter P. *Molecular biology of the cell*. 5th ed. New York: Garland Science, Taylor & Francis group; 2007. p. 1205-66.

(2) Dollinger M, Rosenbaum EH, Tempero M. *Everyone's guide to cancer therapy: how cancer is diagnosed, treated, and managed day to day*. 4 ed. Andrews McMeel Publishing; 2002.

(3) Ferlay J, Shin HRin HR, Bray F., Forman D., Mathers C, Parkin DM. GLOBOCAN 2008 v1.2, Cancer Incidence and Mortality Worldwide: IARC CancerBase No. 10 [Online] Lyon, France: International Agency for Research on Cancer; 2010, Available from:http://globocan.iarc.fr [downloaded 16.04.2012].

(4) Ferlay J, Shin HR, Bray F, Forman D, Mathers C, Parkin DM. Estimates of worldwide burden of cancer in 2008: GLOBOCAN 2008. *Int J Cancer* 2010 December 15;**127**(12):2893-917.

(5) Polyak K. Breast cancer: origins and evolution. *J Clin Invest* 2007 November;**117**(11):3155-63.

(6) Balmain A, Gray J, Ponder B. The genetics and genomics of cancer. *Nat Genet* 2003 March;**33** Suppl:238-44.:238-44.

(7) Le QJ, Caldas C. Micro-RNAs and breast cancer. *Mol Oncol* 2010 June;**4**(3):230-41.

(8) Hanahan D, Weinberg RA. The hallmarks of cancer. *Cell* 2000 January 7;**100**(1):57-70.

(9) Navin NE, Hicks J. Tracing the tumor lineage. *Mol Oncol* 2010 June;**4**(3):267-83.

(10) Nowell PC. The clonal evolution of tumor cell populations. *Science* 1976;**194**(4260):23.

(11) Pardal R, Clarke MF, Morrison SJ. Applying the principles of stem-cell biology to cancer. *Nature Reviews Cancer* 2003;**3**(12):895-902.

(12) Al-Hajj M, Wicha MS, Benito-Hernandez A, Morrison SJ, Clarke MF. Prospective identification of tumorigenic breast cancer cells. *Proceedings of the National Academy of Sciences* 2003;**100**(7):3983.

(13) McCubrey JA, Chappell WH, Abrams SL, Franklin RA, Long JM, Sattler JA et al. Targeting the cancer initiating cell: the Achilles' heel of cancer. *Advances in enzyme regulation* 2011;**51**(1):152.

(14) Hanahan D, Weinberg RA. Hallmarks of cancer: the next generation. *Cell* 2011 March 4;**144**(5):646-74.

(15) Cancer Registry of Norway (2011). Cancer in Norway 2009- Cancer incidence, mortality, survival and prevalence in Norway [online]. Available from: http://www.kreftregisteret.no/Global/Cancer%20in%20Norway/2009/Cancer_in_Norway_2009_trykkversjonen_for_web.pdf, [downloaded 13.03.2012].

(16) Kelsey JL, Berkowitz GS. Breast cancer epidemiology. *Cancer Res* 1988 October 15;**48**(20):5615-23.

(17) Kelsey JL, Gammon MD, John EM. Reproductive factors and breast cancer. *Epidemiol Rev* 1993;**15**(1):36-47.

(18) Solomon E, Berg L, Martin DW. *Biology*. 7th ed. England: Thomson Brooks/Cole; 2005.

(19) Lanigan F, O'Connor D, Martin F, Gallagher WM. Molecular links between mammary gland development and breast cancer. *Cell Mol Life Sci* 2007 December;**64**(24):3159-84.

(20) Sloane E. *Biology of women*. 4 ed. Delmar Pub; 2002.

(21) Virtual Medical Centre (2012), Breast structure [online], Available from: http://www.virtualmedicalcentre.com/anatomy/breast/12, [downloaded: 07.05.2012].

(22) Leonard GD, Swain SM. Ductal carcinoma in situ, complexities and challenges. *J Natl Cancer Inst* 2004 June 16;**96**(12):906-20.

(23) Wist E, Naume B, Lønning PE, Schlichting E. (2012) Blåboka [online], Norwegian breast cancer group (NBCG), Available from: http://www.nbcg.no/nbcg.blaaboka.html, [downloaded: 20.04.2012].

(24) Allred DC, Mohsin SK, Fuqua SA. Histological and biological evolution of human premalignant breast disease. *Endocr Relat Cancer* 2001 March;**8**(1):47-61.

(25) UpToDate. (2012) Breast cancer development [online]. UpToDate, Available from: http://www.uptodate.com/contents/image?imageKey=PI%2F53453&topicKey=PI%2F858&source=see_link&utdPopup=true, [downloaded: 30.04.2012].

(26) Perou CM, Sorlie T, Eisen MB, van de Rijn M, Jeffrey SS, Rees CA et al. Molecular portraits of human breast tumours. *Nature* 2000 August 17;**406**(6797):747-52.

(27) Sorlie T, Perou CM, Tibshirani R, Aas T, Geisler S, Johnsen H et al. Gene expression patterns of breast carcinomas distinguish tumor subclasses with clinical implications. *Proc Natl Acad Sci U S A* 2001 September 11;**98**(19):10869-74.

(28) Singletary SE, Connolly JL. Breast cancer staging: working with the sixth edition of the AJCC Cancer Staging Manual. CA *Cancer J Clin* 2006 January;**56**(1):37-47.

(29) Bland KI, Menck HR, Scott-Conner CE, Morrow M, Winchester DJ, Winchester DP. The National Cancer Data Base 10-year survey of breast carcinoma treatment at hospitals in the United States. *Cancer* 1998 September 15;**83**(6):1262-73.

(30) Ignatiadis M, Sotiriou C. Understanding the molecular basis of histologic grade. *Pathobiology* 2008;**75**(2):104-11.

(31) Elston CW, Ellis IO. Pathological prognostic factors in breast cancer. I. The value of histological grade in breast cancer: experience from a large study with long-term follow-up. *Histopathology* 1991 November;**19**(5):403-10.

(32) Dunnwald LK, Rossing MA, Li CI. Hormone receptor status, tumor characteristics, and prognosis: a prospective cohort of breast cancer patients. *Breast Cancer Res* 2007;**9**(1):R6.

(33) Hudis CA. Trastuzumab--mechanism of action and use in clinical practice. *N Engl J Med* 2007 July 5;**357**(1):39-51.

(34) Murphy CG, Fornier M. HER2-positive breast cancer: beyond trastuzumab. *Oncology (Williston Park)* 2010 April 30;**24**(5):410-5.

(35) de AE, Cardoso F, de CG, Jr., Colozza M, Mano MS, Durbecq V et al. Ki-67 as prognostic marker in early breast cancer: a meta-analysis of published studies involving 12,155 patients. *Br J Cancer* 2007 May 21;**96**(10):1504-13.

(36) Van de Steene J, Soete G, Storme G. Adjuvant radiotherapy for breast cancer significantly improves overall survival: the missing link. *Radiother Oncol* 2000 June;**55**(3):263-72.

(37) Clarke M, Collins R, Darby S, Davies C, Elphinstone P, Evans E et al. Effects of radiotherapy and of differences in the extent of surgery for early breast cancer on local recurrence and 15-year survival: an overview of the randomised trials. *Lancet* 2005 December 17;**366**(9503):2087-106.

(38) Longley DB, Johnston PG. Molecular mechanisms of drug resistance. *J Pathol* 2005 January;**205**(2):275-92.

(39) Foulkes WD, Smith IE, Reis-Filho JS. Triple-negative breast cancer. *New England Journal of Medicine* 2010;**363**(20):1938-48.

(40) Cleator S, Heller W, Coombes RC. Triple-negative breast cancer: therapeutic options. *Lancet Oncol* 2007 March;**8**(3):235-44.

(41) Dent R, Trudeau M, Pritchard KI, Hanna WM, Kahn HK, Sawka CA et al. Triple-negative breast cancer: clinical features and patterns of recurrence. *Clinical Cancer Research* 2007;**13**(15):4429-34.

(42) Haffty BG, Yang Q, Reiss M, Kearney T, Higgins SA, Weidhaas J et al. Locoregional relapse and distant metastasis in conservatively managed triple negative early-stage breast cancer. *J Clin Oncol* 2006 December;**%20;24**(36):5652-7.

(43) Gupta GP, Massague J. Cancer metastasis: building a framework. *Cell* 2006 November 17;**127**(4):679-95.

(44) Fidler IJ. The pathogenesis of cancer metastasis: the 'seed and soil' hypothesis revisited. *Nat Rev Cancer* 2003 June;**3**(6):453-8.

(45) Talmadge JE, Fidler IJ. AACR centennial series: the biology of cancer metastasis: historical perspective. *Cancer Res* 2010 July 15;**70**(14):5649-69.

(46) Chambers AF, Groom AC, MacDonald IC. Dissemination and growth of cancer cells in metastatic sites. *Nat Rev Cancer* 2002 August;**2**(8):563-72.

(47) Luzzi KJ, MacDonald IC, Schmidt EE, Kerkvliet N, Morris VL, Chambers AF et al. Multistep nature of metastatic inefficiency: dormancy of solitary cells after successful extravasation and limited survival of early micrometastases. *Am J Pathol* 1998 September;**153**(3):865-73.

(48) Steeg PS. Metastasis suppressors alter the signal transduction of cancer cells. *Nat Rev Cancer* 2003 January;**3**(1):55-63.

(49) Klein CA. Parallel progression of primary tumours and metastases. *Nat Rev Cancer* 2009 April;**9**(4):302-12.

(50) Koscielny S, Tubiana M, Le MG, Valleron AJ, Mouriesse H, Contesso G et al. Breast cancer: relationship between the size of the primary tumour and the probability of metastatic dissemination. *Br J Cancer* 1984 June;**49**(6):709-15.

(51) Lorusso G, Ruegg C. New insights into the mechanisms of organ-specific breast cancer metastasis. *Semin Cancer Biol* 2012 April 5.

(52) Bernards R, Weinberg RA. A progression puzzle. *Nature* 2002 August 22;**418**(6900):823.

(53) Albini A, Mirisola V, Pfeffer U. Metastasis signatures: genes regulating tumor-microenvironment interactions predict metastatic behavior. *Cancer Metastasis Rev* 2008 March;**27**(1):75-83.

(54) Schmidt-Kittler O, Ragg T, Daskalakis A, Granzow M, Ahr A, Blankenstein TJ et al. From latent disseminated cells to overt metastasis: genetic analysis of systemic breast cancer progression. *Proc Natl Acad Sci U S A* 2003 June 24;**100**(13):7737-42.

(55) Hess KR, Varadhachary GR, Taylor SH, Wei W, Raber MN, Lenzi R et al. Metastatic patterns in adenocarcinoma. *Cancer* 2006 April 1;**106**(7):1624-33.

(56) Paget S. The distribution of secondary growths in cancer of the breast. 1889. *Cancer Metastasis Rev* 1989 August;**8**(2):98-101.

(57) Steeg PS. Tumor metastasis: mechanistic insights and clinical challenges. *Nat Med* 2006 August;**12**(8):895-904.

(58) Hartwell KA, Muir B, Reinhardt F, Carpenter AE, Sgroi DC, Weinberg RA. The Spemann organizer gene, Goosecoid, promotes tumor metastasis. *Proc Natl Acad Sci U S A* 2006 December 12;**103**(50):18969-74.

(59) Thiery JP, Sleeman JP. Complex networks orchestrate epithelial-mesenchymal transitions. *Nat Rev Mol Cell Biol* 2006 February;**7**(2):131-42.

(60) Savagner P, Yamada KM, Thiery JP. The zinc-finger protein slug causes desmosome dissociation, an initial and necessary step for growth factor-induced epithelial-mesenchymal transition. *J Cell Biol* 1997 June 16;**137**(6):1403-19.

(61) Batlle E, Sancho E, Franci C, Dominguez D, Monfar M, Baulida J et al. The transcription factor snail is a repressor of E-cadherin gene expression in epithelial tumour cells. *Nat Cell Biol* 2000 February;**2**(2):84-9.

(62) Yang J, Mani SA, Donaher JL, Ramaswamy S, Itzykson RA, Come C et al. Twist, a master regulator of morphogenesis, plays an essential role in tumor metastasis. *Cell* 2004 June 25;**117**(7):927-39.

(63) Folkman J. Role of angiogenesis in tumor growth and metastasis.: *Elsevier*; 2002 p. 15-8.

(64) Sherwood LM, Parris EE, Folkman J. Tumor angiogenesis: therapeutic implications. *New England Journal of Medicine* 1971;**285**(21):1182-6.

(65) Gewirtz DA, Holt SE, Grant S. Apoptosis, Scenescence and Cancer. Totowa, NJ: *Humana Press Inc*; 2007.

(66) Carmeliet P. Angiogenesis in health and disease. *Nat Med* 2003 June;**9**(6):653-60.

(67) Bergers G, Benjamin LE. Tumorigenesis and the angiogenic switch. *Nat Rev Cancer* 2003 June;**3**(6):401-10.

(68) Medscape, (2012) Complexities in Metastatic Breast Cancer Treatment [online]. Available from: http://www.medscape.org/viewarticle/551140, [downloaded: 30.05.2012].

(69) Hunter T. Signaling--2000 and beyond. *Cell* 2000 January 7;**100**(1):113-27.

(70) Andersen JN, Sathyanarayanan S, Di BA, Chi A, Zhang T, Chen AH et al. Pathway-based identification of biomarkers for targeted therapeutics: personalized oncology with PI3K pathway inhibitors. *Sci Transl Med* 2010 August 4;**2**(43):43ra55.

(71) Hennessy BT, Smith DL, Ram PT, Lu Y, Mills GB. Exploiting the PI3K/AKT pathway for cancer drug discovery. *Nat Rev Drug Discov* 2005 December;**4**(12):988-1004.

(72) Cheng JQ, Godwin AK, Bellacosa A, Taguchi T, Franke TF, Hamilton TC et al. AKT2, a putative oncogene encoding a member of a subfamily of protein-serine/threonine kinases, is amplified in human ovarian carcinomas. *Proc Natl Acad Sci U S A* 1992 October 1;**89**(19):9267-71.

(73) Dillon RL, White DE, Muller WJ. The phosphatidyl inositol 3-kinase signaling network: implications for human breast cancer. *Oncogene* 2007 February 26;**26**(9):1338-45.

(74) Bachman KE, Argani P, Samuels Y, Silliman N, Ptak J, Szabo S et al. The PIK3CA gene is mutated with high frequency in human breast cancers. *Cancer Biol Ther* 2004 August;**3**(8):772-5.

(75) Li J, Yen C, Liaw D, Podsypanina K, Bose S, Wang SI et al. PTEN, a putative protein tyrosine phosphatase gene mutated in human brain, breast, and prostate cancer. *Science* 1997 March 28;**275**(5308):1943-7.

(76) Cheng JQ, Lindsley CW, Cheng GZ, Yang H, Nicosia SV. The Akt/PKB pathway: molecular target for cancer drug discovery. *Oncogene* 2005 November 14;**24**(50):7482-92.

(77) Testa JR, Bellacosa A. AKT plays a central role in tumorigenesis. *Proc Natl Acad Sci U S A* 2001 September 25;**98**(20):10983-5.

(78) Liu AX, Testa JR, Hamilton TC, Jove R, Nicosia SV, Cheng JQ. AKT2, a member of the protein kinase B family, is activated by growth factors, v-Ha-ras, and v-src through phosphatidylinositol 3-kinase in human ovarian epithelial cancer cells. *Cancer Res* 1998 July 15;**58**(14):2973-7.

(79) Blume-Jensen P, Hunter T. Oncogenic kinase signalling. *Nature* 2001 May 17;**411**(6835):355-65.

(80) Cizkova M, Cizeron-Clairac G, Vacher S, Susini A, Andrieu C, Lidereau R et al. Gene expression profiling reveals new aspects of PIK3CA mutation in ERalpha-positive breast cancer: major implication of the Wnt signaling pathway. *PLoS One* 2010 December 30;**5**(12):e15647.

(81) Chan TO, Rittenhouse SE, Tsichlis PN. AKT/PKB and other D3 phosphoinositide-regulated kinases: kinase activation by phosphoinositide-dependent phosphorylation. *Annu Rev Biochem* 1999;**68**:965-1014.:965-1014.

(82) Sarbassov DD, Guertin DA, Ali SM, Sabatini DM. Phosphorylation and regulation of Akt/PKB by the rictor-mTOR complex. *Science* 2005 February 18;**307**(5712):1098-101.

(83) Stambolic V, Suzuki A, de la Pompa JL, Brothers GM, Mirtsos C, Sasaki T et al. Negative regulation of PKB/Akt-dependent cell survival by the tumor suppressor PTEN. *Cell* 1998 October 2;**95**(1):29-39.

(84) Dazert E, Hall MN. mTOR signaling in disease. *Curr Opin Cell Biol* 2011 December;**23**(6):744-55.

(85) Cheng JQ, Jiang X, Fraser M, Li M, Dan HC, Sun M et al. Role of X-linked inhibitor of apoptosis protein in chemoresistance in ovarian cancer: possible involvement of the phosphoinositide-3 kinase/Akt pathway. *Drug Resist Updat* 2002 July;**5**(3-4):131-46.

(86) Knuefermann C, Lu Y, Liu B, Jin W, Liang K, Wu L et al. HER2/PI-3K/Akt activation leads to a multidrug resistance in human breast adenocarcinoma cells. *Oncogene* 2003 May 22;**22**(21):3205-12.

(87) Cell Signal Technology I. (2012) PI3K/Akt pathway [online]. Cell Signaling Technology, Inc, Available from: http://www.cellsignal.com/pathways/akt-signaling.jsp, [downloaded:11.05.2012].

(88) Loos M, Hedderich DM, Friess H, Kleeff J. B7-h3 and its role in antitumor immunity. *Clin Dev Immunol* 2010;**2010**:683875. Epub;%2010 Nov 28.:683875.

(89) Arigami T, Narita N, Mizuno R, Nguyen L, Ye X, Chung A et al. B7-h3 ligand expression by primary breast cancer and associated with regional nodal metastasis. *Ann Surg* 2010 December;**252**(6):1044-51.

(90) Greenwald RJ, Freeman GJ, Sharpe AH. The B7 family revisited. *Annu Rev Immunol* 2005;**23**:515-48.:515-48.

(91) Carreno BM, Collins M. The B7 family of ligands and its receptors: new pathways for costimulation and inhibition of immune responses. *Annu Rev Immunol* 2002;**20**:29-53. Epub;%2001 Oct 4.:29-53.

(92) Chapoval AI, Ni J, Lau JS, Wilcox RA, Flies DB, Liu D et al. B7-H3: a costimulatory molecule for T cell activation and IFN-gamma production. *Nat Immunol* 2001 March;**2**(3):269-74.

(93) Castriconi R, Dondero A, Augugliaro R, Cantoni C, Carnemolla B, Sementa AR et al. Identification of 4Ig-B7-H3 as a neuroblastoma-associated molecule that exerts a protective role from an NK cell-mediated lysis. *Proc Natl Acad Sci U S A 2004* August 24;**101**(34):12640-5.

(94) Leitner J, Klauser C, Pickl WF, Stockl J, Majdic O, Bardet AF et al. B7-H3 is a potent inhibitor of human T-cell activation: No evidence for B7-H3 and TREML2 interaction. *Eur J Immunol* 2009 July;**39**(7):1754-64.

(95) Lemke D, Pfenning PN, Sahm F, Klein AC, Kempf T, Warnken U et al. Costimulatory protein 4IgB7H3 drives the malignant phenotype of glioblastoma by mediating immune escape and invasiveness. *Clin Cancer Res* 2012 January 1;**18**(1):105-17.

(96) Luo L, Chapoval AI, Flies DB, Zhu G, Hirano F, Wang S et al. B7-H3 enhances tumor immunity in vivo by costimulating rapid clonal expansion of antigen-specific CD8+ cytolytic T cells. *J Immunol* 2004 November 1;**173**(9):5445-50.

(97) Zang X, Thompson RH, Al-Ahmadie HA, Serio AM, Reuter VE, Eastham JA et al. B7-H3 and B7x are highly expressed in human prostate cancer and associated with disease spread and poor outcome. *Proc Natl Acad Sci U S A* 2007 December 4;**104**(49):19458-63.

(98) Sun J, Chen LJ, Zhang GB, Jiang JT, Zhu M, Tan Y et al. Clinical significance and regulation of the costimulatory molecule B7-H3 in human colorectal carcinoma. *Cancer Immunol Immunother* 2010 August;**59**(8):1163-71.

(99) Hashiguchi M, Kobori H, Ritprajak P, Kamimura Y, Kozono H, Azuma M. Triggering receptor expressed on myeloid cell-like transcript 2 (TLT-2) is a counter-receptor for B7-H3 and enhances T cell responses. *Proc Natl Acad Sci U S A* 2008 July 29;**105**(30):10495-500.

(100) Chen YW, Tekle C, Fodstad O. The immunoregulatory protein human B7H3 is a tumor-associated antigen that regulates tumor cell migration and invasion. *Curr Cancer Drug Targets* 2008 August;**8**(5):404-13.

(101) Tekle C, Nygren MK, Chen YW, Dybsjord I, Nesland JM, Maelandsmo GM et al. B7-H3 contributes to the metastatic capacity of melanoma cells by modulation of known metastasis-associated genes. *Int J Cancer* 2012 May 15;**130**(10):2282-90.

(102) Liu H, Tekle C, Chen YW, Kristian A, Zhao Y, Zhou M et al. B7-H3 silencing increases paclitaxel sensitivity by abrogating Jak2/Stat3 phosphorylation. *Mol Cancer Ther* 2011 June;**10**(6):960-71.

(103) Promega. (2012), CellTiter-Glo® Luminescent Cell Viability Assay Technical Bulletin protocol [online]. Available from: http://www.promega.com/resources/protocols/technical-bulletins/0/celltiter-glo-luminescent-cell-viability-assay-protocol/, [downloaded: 22.04.2012].

(104) Thermo Fisher Scientific Inc. (2012) BCA Protein Assay Reagent (bicinchoninic acid) [online]. Available from: http://www.piercenet.com/products/browse.cfm?fldID=02020101, [downloaded: 22.04.2012].

(105) Smith PK, Krohn RI, Hermanson GT, Mallia AK, Gartner FH, Provenzano MD et al. Measurement of protein using bicinchoninic acid. *Anal Biochem* 1985 October;**150**(1):76-85.

(106) Life Technologies Corporation. (2012) XCell SureLock® Mini-Cell and XCell II™ Blot Module [online]. Available from: https://products.invitrogen.com/ivgn/product/EI0002?ICID=search-product, [downloaded: 09.05.2012].

(107) Thermo Fisher Scientific Inc. (2012) SuperSignal West Dura Chemiluminescent Substrate [online]. Available from: http://www.piercenet.com/browse.cfm?fldID=01041102, [downloaded: 13.05.2012].

(108) GraphPad Prism. (2012) Introducing dose-response curves [online]. GraphPad Software, Inc., Available from: http://www.graphpad.com/curvefit/introduction89.htm, [downloaded: 22.03.2012].

(109) Neve RM, Chin K, Fridlyand J, Yeh J, Baehner FL, Fevr T et al. A collection of breast cancer cell lines for the study of functionally distinct cancer subtypes. *Cancer Cell* 2006 December;**10**(6):515-27.

(110) Voskoglou-Nomikos T, Pater JL, Seymour L. Clinical predictive value of the in vitro cell line, human xenograft, and mouse allograft preclinical cancer models. *Clin Cancer Res* 2003 September 15;**9**(11):4227-39.

(111) Wenger SL, Senft JR, Sargent LM, Bamezai R, Bairwa N, Grant SG. Comparison of established cell lines at different passages by karyotype and comparative genomic hybridization. *Biosci Rep* 2004 December;**24**(6):631-9.

(112) Vargo-Gogola T, Rosen JM. Modelling breast cancer: one size does not fit all. *Nat Rev Cancer* 2007 September;**7**(9):659-72.

(113) Nardone RM. Curbing rampant cross-contamination and misidentification of cell lines. *Biotechniques* 2008 September;**45**(3):221-7.

(114) Ben-Baruch A. Host microenvironment in breast cancer development: inflammatory cells, cytokines and chemokines in breast cancer progression: reciprocal tumor-microenvironment interactions. *Breast Cancer Res* 2003;**5**(1):31-6.

(115) Vinci M, Gowan S, Boxall F, Patterson L, Zimmermann M, Court W et al. Advances in establishment and analysis of 3D tumour spheroid-based functional assays for target validation and drug evaluation. *BMC Biol* 2012 March 22;**10**(1):29.

(116) Kenny PA, Lee GY, Myers CA, Neve RM, Semeiks JR, Spellman PT et al. The morphologies of breast cancer cell lines in three-dimensional assays correlate with their profiles of gene expression. *Mol Oncol* 2007 June;**1**(1):84-96.

(117) Cailleau R, Olive M, Cruciger QV. Long-term human breast carcinoma cell lines of metastatic origin: preliminary characterization. *In Vitro* 1978 November;**14**(11):911-5.

(118) Ross DT, Scherf U, Eisen MB, Perou CM, Rees C, Spellman P et al. Systematic variation in gene expression patterns in human cancer cell lines. *Nat Genet* 2000 March;**24**(3):227-35.

(119) Ellison G, Klinowska T, Westwood RF, Docter E, French T, Fox JC. Further evidence to support the melanocytic origin of MDA-MB-435. *Mol Pathol* 2002 October;**55**(5):294-9.

(120) You H, Yu W, Sanders BG, Kline K. RRR-alpha-tocopheryl succinate induces MDA-MB-435 and MCF-7 human breast cancer cells to undergo differentiation. *Cell Growth Differ* 2001 September;**12**(9):471-80.

(121) Sellappan S, Grijalva R, Zhou X, Yang W, Eli MB, Mills GB et al. Lineage infidelity of MDA-MB-435 cells: expression of melanocyte proteins in a breast cancer cell line. *Cancer Res* 2004 May 15;**64**(10):3479-85.

(122) Hollestelle A, Nagel JH, Smid M, Lam S, Elstrodt F, Wasielewski M et al. Distinct gene mutation profiles among luminal-type and basal-type breast cancer cell lines. *Breast Cancer Res Treat* 2010 May;**121**(1):53-64.

(123) Zhang Q, Fan H, Shen J, Hoffman RM, Xing HR. Human breast cancer cell lines co-express neuronal, epithelial, and melanocytic differentiation markers in vitro and in vivo. *PLoS One* 2010 March 16;**5**(3):e9712.

(124) Barretina J, Caponigro G, Stransky N, Venkatesan K, Margolin AA, Kim S et al. The Cancer Cell Line Encyclopedia enables predictive modelling of anticancer drug sensitivity. *Nature* 2012 March 28;**483**(7391):603-7.

(125) Garnett MJ, Edelman EJ, Heidorn SJ, Greenman CD, Dastur A, Lau KW et al. Systematic identification of genomic markers of drug sensitivity in cancer cells. *Nature* 2012 March 28;**483**(7391):570-5.

(126) van Kooten TG, Klein CL, Kirkpatrick CJ. Western blotting as a method for studying cell-biomaterial interactions: the role of protein collection. *J Biomed Mater Res* 2001 March 5;**54**(3):385-9.

(127) LoPiccolo J, Blumenthal GM, Bernstein WB, Dennis PA. Targeting the PI3K/Akt/mTOR pathway: effective combinations and clinical considerations. *Drug Resist Updat* 2008 February;**11**(1-2):32-50.

(128) Yang L, Dan HC, Sun M, Liu Q, Sun XM, Feldman RI et al. Akt/protein kinase B signaling inhibitor-2, a selective small molecule inhibitor of Akt signaling with antitumor activity in cancer cells overexpressing Akt. *Cancer Res* 2004 July 1;**64**(13):4394-9.

(129) O'Reilly T, McSheehy PM. Biomarker Development for the Clinical Activity of the mTOR Inhibitor Everolimus (RAD001): Processes, Limitations, and Further Proposals. *Transl Oncol 2010* April;**3**(2):65-79.

(130) Normanno N, Morabito A, De LA, Piccirillo MC, Gallo M, Maiello MR et al. Target-based therapies in breast cancer: current status and future perspectives. *Endocr Relat Cancer* 2009 September;**16**(3):675-702.

(131) Normanno N, Bianco C, De LA, Maiello MR, Salomon DS. Target-based agents against ErbB receptors and their ligands: a novel approach to cancer treatment. E*ndocr Relat Cancer* 2003 March;**10**(1):1-21.

(132) Cancer Network. (2011), Dual HER2 blockade with lapatanib, trastuzumab proves valid in two major trials [online]. UBM Medica, Available from: http://www.cancernetwork.com/conference-reports/sabcs2010/content/article/10165/1756285, [downloaded: 05.05.2012].

(133) Feldman ME, Apsel B, Uotila A, Loewith R, Knight ZA, Ruggero D et al. Active-site inhibitors of mTOR target rapamycin-resistant outputs of mTORC1 and mTORC2. *PLoS Biol* 2009 February 10;**7**(2):e38.

(134) U.S Food and Drug Administration (FDA). (2012), Everolimus (FDA) [online]. Available from; http://www.fda.gov/AboutFDA/CentersOffices/OfficeofMedicalProductsandTobacco/CDER/ucm127799.htm, [downloaded: 03.05.2012].

(135) Boulay A, Zumstein-Mecker S, Stephan C, Beuvink I, Zilbermann F, Haller R et al. Antitumor efficacy of intermittent treatment schedules with the rapamycin derivative RAD001 correlates with prolonged inactivation of ribosomal protein S6 kinase 1 in peripheral blood mononuclear cells. *Cancer Res* 2004 January 1;**64**(1):252-61.

(136) O'Reilly KE, Rojo F, She QB, Solit D, Mills GB, Smith D et al. mTOR inhibition induces upstream receptor tyrosine kinase signaling and activates Akt. *Cancer Res* 2006 February 1;**66**(3):1500-8.

(137) Harrington LS, Findlay GM, Gray A, Tolkacheva T, Wigfield S, Rebholz H et al. The TSC1-2 tumor suppressor controls insulin-PI3K signaling via regulation of IRS proteins. *J Cell Biol* 2004 July;%19;**166**(2):213-23.

(138) Wu R, Hu TC, Rehemtulla A, Fearon ER, Cho KR. Preclinical testing of PI3K/AKT/mTOR signaling inhibitors in a mouse model of ovarian endometrioid adenocarcinoma. *Clin Cancer Res* 2011 December 1;**17**(23):7359-72.

(139) Citri A, Yarden Y. EGF-ERBB signalling: towards the systems level. *Nat Rev Mol Cell Biol* 2006 July;**7**(7):505-16.

(140) Barnett SF, Defeo-Jones D, Fu S, Hancock PJ, Haskell KM, Jones RE et al. Identification and characterization of pleckstrin-homology-domain-dependent and isoenzyme-specific Akt inhibitors. *Biochem J* 2005 January 15;**385**(Pt 2):399-408.

APPENDIX A: Reagents and equipment

The reagents and equipments utilized during cell culturing and drug screening are listed in Table A1, reagents for the Lysis buffer are listed in Table A2 and reagents for Western blot analysis are listed in Table A3.

Table A1. Reagents and equipment used in the drug screening and in cell culturing in general

Name	Vendor	Catalog number
Corning® 100x20mm Petri Dish with Cover	Corning	70165-102
Seriological pipette (1mL)	Sarstedt	86.1251.001
Fisherbrand Disposable Serological Pipettes (5mL)	Fischer Scientific	13-676-10H
Fisherbrand Disposable Serological Pipettes (10mL)	Fischer Scientific	13-676-10J
Fisherbrand Disposable Serological Pipettes (25mL)	Fischer Scientific	13-676-10K
Reagent and centrifuge tube, 15 mL	Sarstedt	62.554.502
Reagent and centrifuge tube, 50 mL	Sarstedt	62.547.254
Bürkner Chamber	Carl Roth GmbH	T730.1
Dulbecco's Modified Eagles Medium	Sigma-Aldrich	D5671
Invitrogen HEPES	Life Technologies	15630056
GIBCO®Glutamax	Life Technologies	35050038
GIBCO® Distilled Phosphate Buffered Saline (PBS)	Life Technologies	14190094
GIBCO® Fetal Bovine Serum (FBS)	Life Technologies	26140-079
GIBCO®Pencillin Streptomyces (Pen-Strep)	Life Technologies	15140-122
0,25% Trypsin-EDTA	Life Technologies	25200-056
GIBCO®GlutaMAX	Life Technologies	35050038
GIBCO®destilled H_2O	Life Technologies	10977-035
Puromycin (10mg/ml)	Sigma-Aldrich	P9620-10ML
Dimethyl Sulfoxide (DMSO)	Thermo Scientific	20688
384 well plates	Greiner bio-one	781098
Drug plates	Medical Biotechnology VTT in Finland	Not commercially avaliable
CTG luminescent cell viability assay	Promega	G7572
Corning incorporated Corning® Costar® 96 well cell culture plate	SIGMA-ALDRICH	CLS3596-50EA
Pierce® BCA Protein Assay Kit	Thermo Scientific	23225
Triciribine (API-2)	SIGMA-ALDRICH	T3830-5MG
Everolimus	SIGMA-ALDRICH	07741-10MGF
Cell scrape	TPP Techno Plastic Products AG	99002

Table A2. Reagents used in the lysis buffer (LB)

Name	Vendor	Catalog number
Sodium orthovanadate Na_3VO_4	SIGMA-ALDRICH	S6508
Pepstatin A	SIGMA-ALDRICH	P4265
cOmplete, Mini Protease Inhibitor Cocktail Tablets (PIC)	Roche	04693124001
phospho-STOP Phosphatase inhibitor cocktail tablets	Roche	04906837001
Phenylmethylsulfonyl fluoride (PMSF)	Roche	11359061001
Aprotinin	SIGMA-ALDRICH	A4529
Leupeptin	SIGMA-ALDRICH	L2884

Table A3. Reagents and equipment used in the Western blot analysis

Name	Vendor	Catalog number
NuPage® Sample Reducing agent (10x)	Life Technologies	NP0009
NuPage® LDS Sample Buffer (4x) Invitrogen™	Life Technologies	NP0008
NuPage® Bis-Tri Polyacrylamid gel	Life Technologies	NP0321BOX
XCell *SureLock*® Mini-Cell and XCell II™ Blot Module	Life Technologies	EI0002
NuPage® MES SDS Running Buffer	Life Technologies	NP0002-02
GIBCO®UltraPure™ 1M Tris-HCI, pH 7.5	Life Technologies	15567-027
Watman™ chromatography papers (3mm)	GE Healthcare	3030-931
Immobilon® Transfer Membranes Polyvinylidene Difluoride (PVDF) (0.45µm pore size)	Millipore	IPVH00010
Tween®20	Merck	8.22184.0500
Albumin for bovine Serum (BSA)	SIGMA-ALDRICH	A3294-50G
Nonfat dry milk (Skimmed milk powder)	TINE	-
SuperSignal West Dura Chemiluminescent Substrate	Thermo Scientific	34075
Tris	Bio-Rad	161-0716
Glycin	Merck	1042010100
SeeBlue®Plus2 Prestained Standard (1x) (Ladder)	Invitrogen	LC5925
Akt antibody	Cell signal	9272
Phospho-Akt (Thr308)	Cell signal	9275L
Phospho-Akt (ser473)	Cell signal	4051S
Phospho-Bad (ser112)	Cell signal	9296S
Phospho-GSK-3β (ser9)	Cell signal	9336S
Phospho-mTOR (Ser2448)	Cell signal	2971S
Phospho-PDK1 (Ser241)	Cell signal	3061
Phospho-elF4E	Cell signal	9741S
Phospho-p70S6K (Thr389)	Cell signal	9206S
Calbiochem® Anti-α-Tubulin Mouse mAb (DM1A)	Millipore	CP06
β-actin	Abcam	ab8229
Human B7-H3	R&D systems	AF1027
Polyclonal Rabbit Anti Goat Immunoglobulins/HRP	Dako	P0449
Polyclonal Rabbit Anti Mouse Immunoglobulins/HRP	Dako	P0161
Polyclonal Goat Anti Rabbit Immunoglobulins/HRP	Dako	P0448

APPENDIX B: Preparation of Lysis Buffer (LB) and Bovine Serum Albumin (BSA) Standard

The stock solution used in the Lysis buffer consisted of 20 mM Tris-HCl pH 7.5, 137 mM NaCl, 100 mM NaF, 10 % Glycerol and 1 % NP-40. The LB was prepared fresh prior to use according to Table B1.

Table B1. Preparation of STOCK solution and Lysis Buffer (LB)

Reagent	**Volume (µL)**
STOCK	714.5
Na_2VO_3 (Vanadate, 200 mM)	2.5
Leupeptin	10
Pepstatin	10
phospho-STOP Phosphatase inhibitor cocktail tablets (10x)	100
Protease Inhibitor Cocktail (PIC) (7x)	143
Phenylmethylsulfonyl fluoride (PMSF)	10
Aprotinin	10
Total Volume	1000

Preparations of the BSA standards were done according to the manufacturer as listed in Table B2.

Table B2. Diluted Albumin (BSA) Standards. Dilution scheme for Standard Test Tube Protocol and Microplate Procedure (Working Range = 20-1500µg/mL) (available from (104).

BSA	**Volume of Diluent (dH_2O) (µL)**	**Volume and source of BSA (µL)**	**Final BSA Concentration (µg/mL)**
A	125	375 of Stock BSA	1500
B	325	325 of Stock BSA	1000
C	175	175 of vial A dilution	750
D	325	325 of vial B dilution	500
E	325	325 of vial C dilution	250
F	325	325 of vial D dilution	125